Characterisation of a Novel Subtilase Cytotoxin from Shiga Toxigenic *Escherichia coli*

Damien Christopher Chen Sau Chong

A thesis submitted in fulfilment of the requirements
for the degree of Doctor of Philosophy

School of Molecular and Biomedical Science
Discipline of Microbiology and Immunology
The University of Adelaide
Australia 5005

October 2008

Chapter 1
Introduction

1.1 Shiga Toxigenic *Escherichia coli*

Escherichia coli is the predominant facultative anaerobe that colonises the human infant gastrointestinal tract within hours of birth (Savage, 1977; Nataro and Kaper, 1998). While *E. coli* generally remain benign in the intestinal lumen, the contravention of the gastrointestinal barrier permits infection even by commensal *E. coli* strains (e.g. peritonitis). Similarly, *E. coli* may acquire specific virulence factors, which confers their ability to adapt to highly specific niches and induce a wide range of diseases that may be localised to the mucosal surfaces or become systemic. Shiga toxigenic *Escherichia coli* (STEC) is one such pathotype of *E. coli* that has acquired its major virulence attribute (the ability to produce Shiga toxin [Stx]) presumably via lateral gene transfer (O'Brien *et al.*, 1984; Schmidt, 2001).

1.1.1 Origins of Synonymous Nomenclature

The diverse strains of *E. coli* are characterised by their O (lipopolysaccharide [LPS]) and H (flagellar) antigens, which are used to define serogroup (based on the O antigen) and serotype (O and H antigens) classifications (Nataro and Kaper, 1998). While Keusch *et al.* (1972) observed that the Stx toxin from *Shigella dysenteriae* type 1 (Shiga's bacillus) could contribute to the bloody diarrhoea presented by patients with bacillary dysentery, STEC were not discovered until a preliminary report by O'Brien *et al.* (1977) demonstrated the capacity for rabbit anti-Stx antisera to neutralise a cytotoxin made by certain *E. coli* strains. Consequently, these pathogens were referred to as Shiga-like toxigenic *E. coli* (SLTEC or STEC). The Vero toxigenic *E. coli* (VTEC) nomenclature originated from observations in the same year by Konowalchuck *et al.* (1977), in which the particular strains of diarrhoeagenic *E. coli* produced a toxin that was cytotoxic to Vero (African green monkey kidney) cells.

It was subsequently observed by O'Brien *et al.* (1983) that a Shiga-like toxin produced by *E. coli* strain O157:H7 was identical to the Vero cytotoxin produced by the same strain described by Johnson *et al.* (1983). Molecular genetics studies found that the primary structure of Stx1 (of *E. coli*) differs from Stx (of Shiga's bacillus) by none or only one amino acid (Strockbine *et al.*, 1988; Takao *et al.*, 1988). Hence, as Vero cytotoxins and Shiga-like toxins produced by *E. coli* are synonymous, and due to their homology with the cytotoxin from Shiga's bacillus, the Shiga toxin (Stx) nomenclature will be used as opposed to Vero cytotoxin (VT) in this text for the purpose of consistency.

1.1.2 Spectrum and Aetiology of Disease

Human STEC infections may present with a wide range of symptoms including uncomplicated or bloody diarrhoea, severe abdominal pain and haemorrhagic colitis. While some individuals infected with STEC may remain asymptomatic despite high levels of organisms and free toxin in the patient's stool (Edelman *et al.*, 1988; Brian *et al.*, 1992), others progress to potentially fatal systemic sequelae including thrombotic thrombocytopenic purpura (TTP), and haemolytic uraemic syndrome (HUS) (Karmali, 1989; Gyles, 1992; Paton and Paton, 1998). Karmali, *et al.* (1985) first reported the association between STEC infection and HUS, which is characterised by a triad of acute renal failure, thrombocytopenia and microangiopathic haemolytic anaemia. These clinical manifestations have long been considered to be directly attributable to effects of Stx on endothelial cells (Paton and Paton, 1998). STEC infection is the leading cause of HUS and accounts for approximately 90% of reported cases (Rose and Chant, 1998). Approximately 30% of those who recover from STEC-induced HUS suffer permanent disabilities including chronic renal deficiency and extrarenal complications such as

diabetes, hypertension and psychological and neurological impairments (Paton and Paton, 1998).

Although infection has been reported in all age groups, infants, young children and elderly people have a higher incidence of disease, with STEC being the most common cause of acute renal failure in the paediatric population (Rowe *et al.*, 1994; Elliott *et al.*, 2001). It is possible that such age-related differences are due to the immunological naïvety of the young and the declining immune system of the elderly. Additionally, the age distribution may be a consequence of age-related differences in toxin receptor expression.

1.1.3 Epidemiology

STEC commonly reside in the intestines of livestock, usually resulting in asymptomatic carriage in adult cattle while inducing diarrhoea in calves (Ørskov *et al.*, 1987; Montenegro *et al.*, 1990; Wells *et al.*, 1991; Beutin *et al.*, 1993). Furthermore, Beutin *et al.* (1993) have reported the presence of STEC in at least six other species of healthy domestic animals including cats and dogs. Accordingly, it is acknowledged that the faeces of infected animals frequently harbour the pathogen and represent the primary source of infection in humans. It should be noted, however, that not all STEC strains appear to be pathogenic to humans (Paton and Paton, 1998; Elliott *et al.*, 2001; Kaper *et al.*, 2004). The transmission of STEC to humans is frequently due to faecal contamination of consumables such as meat and dairy products (contaminated during animal slaughter or processing) and fruits and vegetables (from manure used as fertiliser and contaminated water). Other reservoirs include drinking and swimming water and it is estimated that approximately 20% of human STEC infections are due to person-to-person transmission.

The infectious dose for STEC in susceptible humans may be very low (of the order of 1 – 200 cfu) (Paton *et al.*, 1996; Griffin, 1998) and is similar to that for *Shigella* species. Furthermore, it is consistent with frequent person-to-person transmission reported during outbreaks (Bell *et al.*, 1994; Rowe *et al.*, 1994) and in the clinical setting (Begaud and Germani, 1992). The Centers for Disease Control has estimated O157:H7 (the most common STEC serotype in many parts of the world) causes an annual 20,000 infections in the United States with approximately 250 deaths.

Initially, it was believed that, although most outbreaks of STEC infection have been associated with O157:H7, this did not necessarily reflect the predominance of this serotype in the community. It was thought possible that reports of other outbreak-associated serotypes were underestimated as they were more difficult to isolate than O157:H7 (Karmali, 1989; Paton and Paton, 1998). Indeed, many other STEC serotypes are known to have caused diarrhoea, haemorrhagic colitis and HUS in humans and such conditions may also arise from simultaneous infection by multiple serotypes (Bopp *et al.*, 1987; Bokete *et al.*, 1993; Paton *et al.*, 1996). However, it is now generally accepted that O157:H7 is the most common serotype in Canada, United States, United Kingdom and Japan, whereas in Latin America, continental Europe and Australia non-O157:H7 serotypes are more prevalent (Bell *et al.*, 1994; Waters *et al.*, 1994; Ahmed and Donaghy, 1998; Caprioli and Tozzi, 1998; Griffin, 1998; López *et al.*, 1998; Robins-Browne *et al.*, 1998; Smith *et al.*, 1998; Spika *et al.*, 1998; Paton *et al.*, 1999; Tuttle *et al.*, 1999; Elliott *et al.*, 2001). Reasons for this geographical distribution of serotypes have yet to be elucidated.

Due to the rapid onset and severity of disease, large outbreaks of gastrointestinal disease caused by STEC have the potential to overwhelm acute health care resources, even in developed countries (Karmali, 1989; Bell *et al.*, 1994; Waters *et al.*, 1994; Paton

et al., 1996; Tuttle *et al.*, 1999). The largest outbreak to date occurred in Sakai, Japan in July 1996 when schoolchildren and staff consumed uncooked white radish sprouts contaminated with *E. coli* O157:H7 (Swinbanks, 1996; Michino *et al.*, 1998). Over 8,100 cases were reported, resulting in 619 hospitalisations, 106 progressing to HUS and three deaths.

1.1.4 Pathogenesis and Virulence Factors

The acid resistance of STEC is mediated by the stationary phase sigma factor *rpoS* thereby allowing the stationary phase organisms to survive in environments below pH 2.5 and accordingly, the acidity of the stomach (Gorden and Small, 1993). The pathogen establishes colonisation of the lower small intestine and colon by adherence to epithelial cells and unlike shigellae, do not invade the epithelium to any significant extent (Nataro and Kaper, 1998). While STEC may comprise more than 90% of the gut flora in the early stages of infection, the exact means by which this is achieved are not entirely understood. The most detailed knowledge of an adherence mechanism is of the formation of attaching-effacing (A/E) lesions on enterocytes (Francis *et al.*, 1986; Sherman *et al.*, 1988), which appear to be analogous to A/E lesions formed by enteropathogenic *E. coli* (EPEC) strains (Donnenberg *et al.*, 1997). The genes required for A/E lesions are encoded on the locus for enterocyte effacement (LEE) and include *eae*, which encodes the outer membrane protein mediator of attachment, intimin (Donnenberg *et al.*, 1997; Lai *et al.*, 1997), the translocated intimin receptor, Tir (Kenny *et al.*, 1997) and *sep* genes that encode a Type III secretion apparatus to inject proteins such as Tir into the host cell membrane. The lesions are characterised by ultra-structural changes including loss of enterocyte microvilli and intimate adherence of the pathogen to the cell surface. Furthermore, cytoskeletal components including polymerised actin accumulate beneath the site of attachment, thereby forming a pedestal (Knutton *et al.*,

1989). In addition to mediating adherence, the lesions may contribute to STEC-associated diarrhoea by altering ion transport channels and opening tight junctions, which increases intestinal epithelial permeability and induces a mass secretory state in the host manifested as diarrhoea (Knutton *et al.*, 1989).

Stx is one of the major virulence determinants of STEC, which in conjunction with host inflammatory mediators is capable of causing considerable endothelial damage (Nataro and Kaper, 1998; Paton and Paton, 1998). In the 1980s it was determined that genes encoding Stx usually reside on lambdoid phages in *E. coli* (Scotland *et al.*, 1983; Smith *et al.*, 1983; O'Brien *et al.*, 1984; Strockbine *et al.*, 1986; O'Brien *et al.*, 1989) whereas the pig oedema disease toxin, Stx2e, and Stx from Shiga's bacillus were found to be chromosomally encoded (Strockbine *et al.*, 1988; Weinstein *et al.*, 1988).

In humans, Stx recognises the oligosaccharide component of globotriaosyl ceramide (Gb_3) (Lingwood *et al.*, 1987) and differences in Stx receptor expression among various cell types determines host specificity and tissue trophism of disease (Zopf and Roth, 1996; Karlsson, 1998). Indeed, high concentrations of membrane-bound Gb_3 are found in the cortical region of human kidneys, which is the main location of lesions in HUS patients (Boyd and Lingwood, 1989). When Stx attacks tubule epithelial cells, in addition to possibly inducing apoptosis (Cherla *et al.*, 2003), the affected cells and macrophages release TNFα (Hughes *et al.*, 1998; Hughes *et al.*, 2001). *In vitro* studies demonstrated that TNFα increases Gb_3 surface expression by upregulating a galactosyltransferase required for Gb_3 synthesis (van de Kar *et al.*, 1992; van de Kar *et al.*, 1995). In particular, TNFα upregulates surface Gb_3 on glomerular microvascular endothelial cells thereby increasing Stx sensitivity and precipitating HUS (Monnens *et al.*, 1998). Furthermore, Louise *et al.* (1995) reported that sodium butyrate

increased Gb_3 expression and subsequent sensitisation to Stx in human umbilical vein endothelial cells, suggesting that endothelial cell exposure to colonic butyrate during STEC infection may contribute to intestinal damage and ultimately haemorrhagic colitis.

1.2 Bacterial AB_5 Protein Toxins

Pathogenic bacteria deploy a diverse array of toxins in order to damage their hosts, and as a consequence, cause massive global morbidity and mortality in animals and humans. The different types of toxins include membrane-damaging toxins, super-antigens and AB toxins. The latter group incorporate AB_5 toxins, characterised by a pentameric B subunit, which recognises and binds to specific glycan receptors on the surface of eukaryotic cells and directs the internalisation of an enzymatic A subunit that subsequently disrupts essential host cell processes (Fan *et al.*, 2000). Until recently, three classes of AB_5 toxins have been characterised and are exemplified by Cholera toxin (Ctx) and the family of related heat labile enterotoxins (LT), Stx, and pertussis toxin (Ptx) (Sixma *et al.*, 1991; Fraser *et al.*, 1994; Stein *et al.*, 1994a). They are produced by *Vibrio cholera* and enterotoxigenic *E. coli* (ETEC), *S. dysenteriae* and STEC, and *Bordetella pertussis*, respectively, and in each case, are the major virulence factor of the bacteria that deploys them.

1.2.1 Toxin Recognition of Host Cell Oligosaccharides

Mammalian cells display a range of oligosaccharide moieties in the context of surface glycoproteins and glycolipids which can mediate and modulate a wide variety of biological functions (Varki, 1993; Karlsson, 1998). Variations in the sugar subunit sequence, the linkages which join them and their potential to form linear and branched structures allow for an extensive array of glycan configurations that can be expressed on

these glycoconjugates. Unlike DNA, RNA and proteins, oligosaccharide biosynthesis is not dependent on a template, but follows a sequential assembly pathway in which a change in a single enzyme involved in the ER-Golgi biosynthetic pathway can result in a marked change in the glycans of a large number of glycoproteins and glycolipids (Varki, 1998). Host cell glycoconjugates are often targeted by pathogens (such as bacteria, viruses, protozoans and yeasts) and it is understood that binding to these carbohydrates by microbial products, including bacterial AB_5 protein toxins, contributes significantly to the pathogenesis of disease (Fishman, 1982; Lingwood *et al.*, 1987). Such recognition is often highly specific in that the toxin will only bind to a host cell surface if it possesses a complementary receptor. Consequently, it is understood that the diverse and discriminatory glycosylation of host tissues influences not only the range of species a toxin can affect, but also the site at which disease can be established (Zopf and Roth, 1996; Karlsson, 1998).

The B subunits of AB_5 toxins recognise specific glycan configurations often in the context of membrane-bound glycolipids (Merritt and Hol, 1995). The glycolipids are molecules that comprise one or more glycosidically-linked sugar residues which are presented on the target cell surface and covalently attached to a lipid domain that is anchored in the outer membrane. The receptors bound by AB_5 toxins belong to the neutral glycosphingolipid (GSL) group or the acidic GSL subgroup known as gangliosides (GGS), which contain at least one acidic residue such as N-acetylneuraminic acid (Neu5Ac), also known as sialic acid (Svennerholm, 1980; Smith *et al.*, 2004). The lipid portion of GSL receptors is a ceramide which comprises a sphingosine backbone and fatty acid tails (Lingwood, 1996). A selected list of AB_5 toxin glycolipid receptors is presented in Table 1.1.

Binding of Ctx to the extracellular glycan domain of monosialo-GGS GM_1 was shown to be accomplished by CtxB (Figure 1.1a) (Orlandi and Fishman, 1993). Studies employed antisera against specific Ctx subunits and demonstrated that antisera against the A subunit was unable to prevent Ctx targeting the cell surface, despite binding to the holotoxin and only anti-CtxB antisera inhibited Ctx membrane recognition. Hence, CtxB is sufficient to bind GM_1 with CtxA facing away from the membrane. Recognition of GM_1 by the CtxB homopentamer is achieved by active sites that reside at the junctions between CtxB monomers (Jobling and Holmes, 1991). Site-directed mutagenesis studies have demonstrated that both adjacent CtxB subunits provide critical amino acid residues to produce a binding cleft, thereby facilitating the simultaneous recognition of up to five GM_1 receptor molecules (Jobling and Holmes, 1991). Furthermore, these results were both confirmed by the elucidation of the crystal structure of CtxB complexed with GM_1 (Merritt et al., 1994).

Table 1.1: Selected glycan receptors recognised by AB_5 toxins.

Toxin	Pathogen	Receptor	Reference
Ctx	*V. cholera*	GM_1	(Fishman, 1982)
LT-I LT-IIa	ETEC	GM_1	(Fishman, 1982)
LT-IIb	ETEC	GD_{1a}	(Fukuta *et al.*, 1988)
Ptx	*B. pertussis*	Lactosylceramide Neu5Acα(2→3)Galβ	(Saukkonen *et al.*, 1992) (Stein *et al.*, 1994b)
Stx1 Stx2 Stx2c	*S. dysenteriae*, STEC	Gb_3	(Lingwood *et al.*, 1987)
Stx2e	STEC	Gb_4	(DeGrandis *et al.*, 1989)

a

PDB ID: 1S5E (O'Neal *et al.*, 2004).

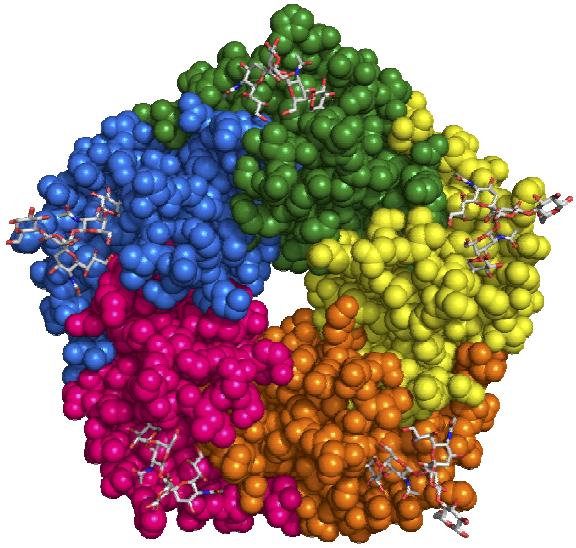

PDB ID: 3CHB (Merritt *et al.*, 1998).

b

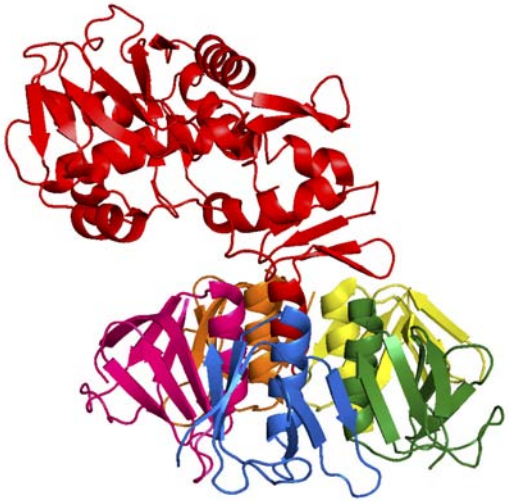

PDB ID: 1R4P (Fraser *et al.*, 2004).

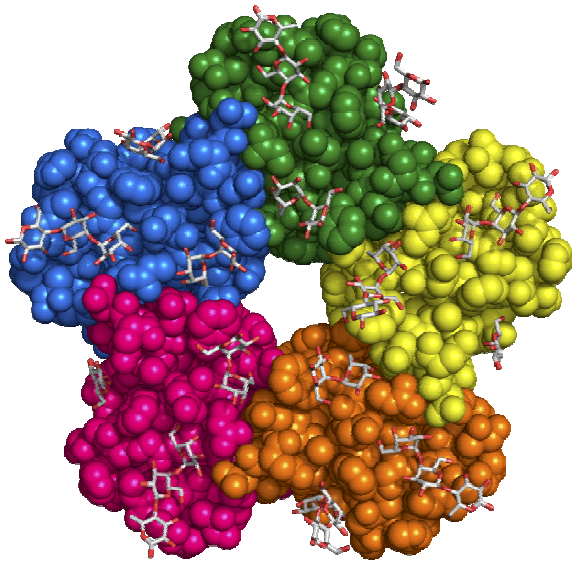

PDB ID: 1BOS (Ling *et al.*, 1998).

Figure 1.1: AB_5 toxin structures.

The structures of Ctx (a) and Stx2 (b) as determined by X-ray diffraction. Ribbon structures of the holotoxins (left) are viewed sideways with eznymatic A subunits in red and five identical B monomers facing down. Volumetric structures of the cell-binding B pentamers alone (right) are viewed from below, complexed with their specific carbohydrate receptors (geometric sticks). The CtxB pentamer recognises upto five GM_1 molecules, whereas StxB can bind a maxmimum of 15 Gb_3 receptors. Files were obtained from the Research Collaboratory for Structural Bioinformatics Protein Data Bank and rendered using PyMOL v0.99edu8 (DeLano Scientific LLC, Palo Alto, CA) with ray tracing enabled.

All forms of Stx that affect humans comprise a pentameric B subunit that mediates adherence to the host cell surface by recognising the carbohydrate portion of the GSL Gb_3 (Figure 1.1b) (Lingwood *et al.*, 1987). Stx2e, which is associated with piglet oedema disease, binds to globotetraosyl ceramide (Gb_4) (Weinstein *et al.*, 1988; DeGrandis *et al.*, 1989; Gyles, 1992). Despite the distinct glycolipid binding specificity of the oedema disease toxin, the mechanism of toxicity is the same as those that recognise Gb_3. Unlike CtxB, however, StxB does not form functional binding pockets at the junctions of adjacent monomers, but rather, X-ray crystallography revealed that each monomer harbours three active binding sites, allowing a single StxB pentamer to associate with a maximum of 15 receptors (Ling *et al.*, 1998; Bast *et al.*, 1999).

Unlike Ctx and Stx, Ptx comprises an enzymatic S1 and a binding heteropentamer of S2, S3, S5 and two S4 subunits (Stein *et al.*, 1994a; Merritt and Hol, 1995) (Figure 1.2). Recognition of target cell surfaces by Ptx is facilitated by the S2 and S3 subunits of the B oligomer (Saukkonen *et al.*, 1992; Stein *et al.*, 1994b). Saukkonen *et al*. (1992) suggest that S2 recognises ciliary lactosylceramide and S3 binds a macrophage GGS. Stein *et al*. (1994b), however, present the crystal structure of Ptx complexed with the distal sialic acid of the decasaccharide found on transferrin. While the subcellular transport of Ptx has been described (Plaut and Carbonetti, 2008), due to the heteropentameric structure of the B oligomer and the lack of corroborating evidence to establish the true receptor, Ptx was not used in the current study.

The presence of a toxin receptor on the cell surface is not sufficient to confer toxin sensitivity (Jacewicz *et al.*, 1994). By fusing Chinese Hamster Ovary cells, which are refractory to Stx and deficient of surface Gb_3, with liposomes containing Gb_3 Jacewicz *et al*. (1994) showed that the addition of Gb_3 into a target cell membrane increased its ability to bind Stx, but did not render the cells sensitive to the toxin.

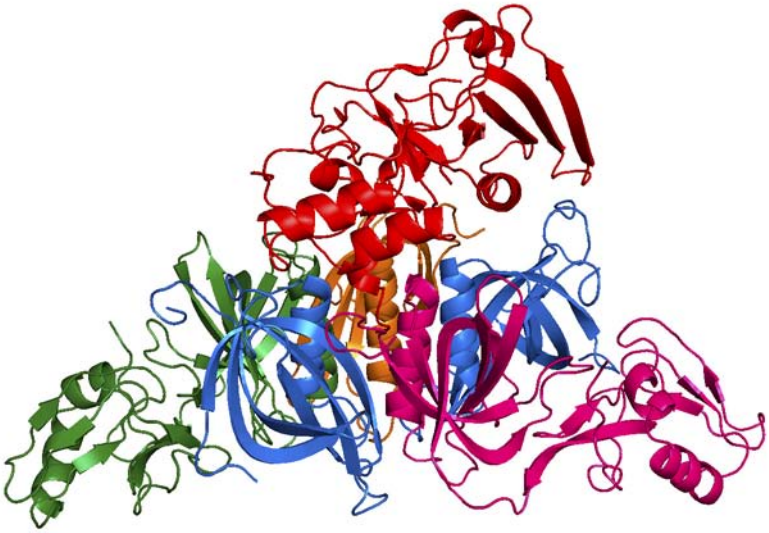

PDB ID: 1PRT (Stein *et al.*, 1994a).

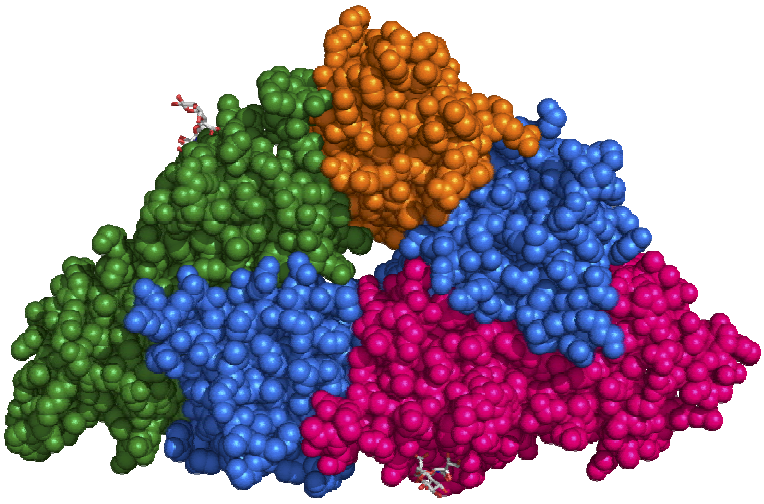

PDB ID: 1PTO (Stein *et al.*, 1994b).

Figure 1.2: Ptx structure.

The structure of Ptx as determined by X-ray diffraction. The ribbon structure of the holotoxin (top) is viewed sideways with the enzymatic S1 subunit in red and S2 – S5 monomers facing down. The volumetric structure of the cell-binding S2 – S5 heteropentamer alone (bottom) is viewed from above, complexed with Neu5Acα(2→3)Galβ (geometric sticks). Note the two identical S4 subunits in blue. Structural data of Ptx bound to lactosylceramide were unavailable. Files were obtained from the Research Collaboratory for Structural Bioinformatics Protein Data Bank and rendered using PyMOL v0.99edu8 (DeLano Scientific LLC, Palo Alto, CA) with ray tracing enabled.

Although the carbohydrate domain is crucial for the targeting of AB_5 toxins to the cell surface, the ceramide composition has also been implicated in the affinity of a toxin for its complementary glycolipid receptor and subsequent intracellular trafficking (Kannagi *et al.*, 1982; Crook *et al.*, 1986; Pellizzari *et al.*, 1992; Arab and Lingwood, 1998; Lingwood, 2000; Mayor and Riezman, 2004). Semi-synthetic Gb_3 with a fatty acyl chain consisting of either 12 or 14 carbons exhibited minimal Stx binding. However, Gb_3 with fatty acid chains comprising 16 to 22 carbons exhibited up to 10-fold greater affinity, while Stx binding declined for Gb_3 with chains greater than 22 carbons (Boyd *et al.*, 1994; Kiarash *et al.*, 1994). Further Gb_3 isotypes were produced by varying the degree of unsaturation; those with an unsaturated fatty acid chain exhibited increased Stx affinity relative to those with saturated chains for all hydrocarbon chain lengths (Kiarash *et al.*, 1994). In the same study, receptor-deficient VT500 Daudi lymphoma cells were fused with liposomes containing Gb_3 isotypes. Cells reconstituted with Gb_3 harbouring unsaturated 22- and 18-carbon fatty acyl chains possessed the greatest capacity to sensitise cells to Stx1 and Stx2c, respectively. Additionally, when displayed in an auxiliary lipid matrix comprising phosphatidylcholine and cholesterol, the binding capacities for Stx of these isotypes increased compared to their presentation in a thin layer chromatography (TLC) toxin overlay assay (Crook *et al.*, 1986; Kiarash *et al.*, 1994). The increased avidity is not surprising as the supporting matrix is a better representation the cell membrane environment, thus allowing optimal positioning and orientation of globotriose residues for Stx.

Structural heterogeneity of the GM_1 ceramide domain can determine the association of GM_1 with lipid rafts (clustered membrane microdomains containing glycosphingolipids and cholesterol); an association that is necessary for subsequent Ctx trafficking (Simons and Ikonen, 1997; Wolf *et al.*, 1998; Wolf *et al.*, 2002; Chinnapen

et al., 2007). Ctx-induced chloride secretion was delayed and diminished in human intestinal T84 cells by reversibly depleting cholesterol with 2-hydroxypropyl-β-cyclodextrin or methyl-β-cyclodextrin (MβCD), indicating that the ability for the GM_1 lipid moiety to associate with cholesterol, and thus lipid rafts, affects the efficiency of Ctx trafficking and cytotoxicity.

1.2.2 Cholera Toxin

Cholera toxin (Ctx) consists of a 29.4-kDa enzymatic A subunit (CtxA) and five identical 11.6-kDa B subunit peptides (CtxB) that form a pentameric ring (Orlandi and Fishman, 1993; Merritt *et al.*, 1994). Ctx and LT-I have an 80% sequence homology in both the A and the B subunits, whereas Ctx shares lower sequence homology with LT-II (less than 56% and 11% for the A and B subunits, respectively).

Upon its release into the gut lumen, Ctx binds to GM_1 displayed on the surface of intestinal epithelial cells (Fishman, 1982; Griffiths *et al.*, 1986; Spangler, 1992; Merritt *et al.*, 1994). After associating with lipid rafts, the toxin-receptor complex is internalised by several routes. Studies have shown that Ctx exploits caveolae- and/or clathrin-dependent endocytosis, depending on the cell line and Caveolin-1 expression (Nichols, 2002; Singh *et al.*, 2003; Hansen *et al.*, 2005). Orlandi and Fishman (1998) proposed that Ctx uptake may depend on lipid rafts rather than a specific morphological structure, while Shogomori *et al*. (2001) showed that, despite associating with lipid rafts in hippocampal neurons, Ctx was internalised via a raft-independent pathway. Furthermore, Sandvig and van Deurs (authors' reply in Fishman and Orlandi (2003)) report that Ctx uptake may also occur via a mechanism independent of caveolae, clathrin and cholesterol.

Regardless of the pathway exploited, an endogenous protease of apically-derived endosomes cleaves Ctx into $CtxA_1$ and $CtxA_2$-B which remain tethered by a disulphide

bridge (Lencer *et al.*, 1997). Ctx is subsequently transported via the *trans*-Golgi network (TGN) and the Golgi to the endoplasmic reticulum (ER) where the disulphide bridge is reduced by the redox-dependent ER chaperone protein disulfide isomerase (PDI) releasing an enzymatically active $CtxA_1$ (Orlandi and Fishman, 1998; Tsai *et al.*, 2001). CtxB remains bound to GM_1 in the ER membrane (Fujinaga *et al.*, 2003) while the unfolded $CtxA_1$ chain is then targeted to the ER lumen with PDI, where it is subsequently oxidised by the enzyme Ero1 and committed to retrotranslocation across the ER membrane, facilitated by proteins involved in the ER stress response including Derlin-1 and possibly Derlin-2 and BiP (Tsai and Rapoport, 2002; Bernardi *et al.*, 2007; Dixit *et al.*, 2008). $CtxA_1$ is then transported through the Sec61 channel into the cytosol (Schmitz *et al.*, 2000; Teter *et al.*, 2002) and catalyses the ADP-ribosylation of an arginine of $G_s\alpha$ (the α subunit of the stimulatory heterotrimeric G protein) (Gill, 1975; Gill and Richardson, 1980). This causes the constitutive activation of adenylyl cyclase, increasing the intracellular level of cyclic adenosine monophosphate (cAMP), and induces intestinal chloride secretion, leading to the mass secretory state that is characteristic of cholera.

1.2.3 Shiga Toxin

Stx comprises a single 32-kDa catalytic A subunit StxA and five 7.7-kDa monomers that associate in a ring-like structure to form a lectin B subunit (StxB) (Middlebrook and Dorland, 1984; O'Brien and Holmes, 1987; Merritt and Hol, 1995). As mentioned in Section 1.1.1, the Stx1 from STEC is virtually identical to the toxin deployed by Shiga's bacillus (differing by only one amino acid in the A subunit). A second Stx type produced by STEC had only a 56% identity for both A and B subunits when compared to the other Shiga toxins (Jackson *et al.*, 1987) and thus, referred to as Stx2. Variants of both Stx1 and Stx2 have been reported from human STEC isolates

with the most prominent being Stx2c and Stx2d (Oku *et al.*, 1989; Gannon *et al.*, 1990; Ito *et al.*, 1990; Schmitt *et al.*, 1991; Meyer *et al.*, 1992; Paton *et al.*, 1992; Lin *et al.*, 1993; Paton *et al.*, 1993a; Paton *et al.*, 1993b; Paton *et al.*, 1995). The toxin variant associated with piglet oedema disease is designated Stx2e (Gyles *et al.*, 1988; Weinstein *et al.*, 1988).

Upon secretion into the gut lumen, Stx traverses the epithelium via a transcellular, rather than a paracellular, pathway into the bloodstream without apparent cellular disruption (Acheson *et al.*, 1996). However, epithelial damage mediated by Stx, LPS or inflammatory cytokines may also promote toxin translocation (Paton and Paton, 1998). Upon binding to the target cell surface displaying Gb_3 (or Gb_4 in the case of Stx2e) Stx is internalised by receptor-mediated endocytosis. In humans, Gb_3 is found most frequently on tubule epithelial cells and on microvascular endothelium of the kidneys, gut, pancreas and brain. In cell lines refractory to Stx cytotoxicity, the Stx-containing endocytic compartments are fused to lysosomes and the toxin is degraded (Sandvig and van Deurs, 1996). However, in susceptible cells, including Vero cells, Stx is internalised from the cell surface by both cholesterol- and clathrin-dependent endocytic routes and undergoes retrograde transport via the Golgi apparatus to the ER (Sandvig *et al.*, 1989; Sandvig *et al.*, 1992; Sandvig *et al.*, 1994). Furthermore, Stx activates the tyrosine kinase Syk, which subsequently phosphorylates clathrin heavy chain and up-regulates Stx uptake (Lauvrak *et al.*, 2006). Similar to CtxA, StxA is nicked into two fragments (which remain linked by a disulfide bond) by an ER membrane-bound protease, furin (Garred *et al.*, 1995). Subsequent reduction of the disulfide bond releases the 27-kDa RNA *N*-glycosidase A1 fragment from the 4-kDa A2 fragment into the cytosol (Sandvig and van Deurs, 1996), allowing the A1 fragment to cleave a specific adenine base in the 28S ribosomal RNA (Endo *et al.*, 1988; Saxena *et*

al., 1989; Skinner and Jackson, 1997). Consequently, depurination of ribosomal RNA inhibits peptide elongation and protein synthesis, ultimately causing cell death.

1.3 Adjuvanticity of Cholera Toxin

In addition to their role as major virulence factors and causative agents of diarrhoea, Stx, Ctx and the related LT have significant immunological properties (Del Giudice and Rappuoli, 1999; Williams *et al.*, 1999; Haicheur *et al.*, 2000; Ohmura-Hoshino *et al.*, 2004; Holmgren and Czerkinsky, 2005). Although studies with Stx are limited, systemic immunisation with Ctx induces a strong anti-toxin immune response and, when administered at doses below that required to elicit clinical symptoms, can function as a strong mucosal adjuvant (Williams *et al.*, 1999). Initially demonstrated by Glenn *et al*. (1998a), Ctx also possesses systemic adjuvanticity upon transcutaneous immunisation and has subsequently been shown to enhance both mucosal IgA and serum IgG responses to a topical application of a co-administered antigen to the skin of mice and humans (Glenn *et al.*, 2000; Gockel *et al.*, 2000), indicating that Ctx may be potentially used as an adjuvant in mucosal and parenteral immunisation.

The glycolipid affinity of CtxB for GM_1 nevertheless raises concerns over the possibility of host neuronal damage, as high levels of GM_1 are expressed in the central nervous system. CtxB conjugated to horseradish peroxidase (CtxB-HRP) has been exploited as a neuronal tracer in rats upon intraperitoneal (i.p.) delivery (Havton and Broman, 2005), and after intranasal (i.n.) administration in mice, both Ctx and CtxB accumulated in the main olfactory nerves, epithelia and olfactory bulbs (van Ginkel *et al.*, 2000; Campos *et al.*, 2003). A toxicologically acceptable variant of Ctx is therefore highly desired when exploiting its adjuvant properties. In general, the attenuation of Ctx toxicity correlates with reduced adjuvanticity. However, site-directed mutations of Ctx and LT in other studies have demonstrated the ability to separate toxicity from immuno-

potentiating effects; that is, to abolish enzymatic activity while retaining adjuvanticity (Pizza *et al.*, 2001; Holmgren and Czerkinsky, 2005).

The development of non-toxic Ctx variants for use as adjuvants has been approached by various methods. These include mutating the active (catalytic) site of CtxA, site-directed mutagenesis targeting the link between CtxA1 and CtxA2 to prevent proteolytic nicking, and blocking the active site by peptide extension of CtxA (Douce *et al.*, 1995; Pizza *et al.*, 2001; Lu *et al.*, 2002; Sanchez *et al.*, 2002). Indeed, a non-toxic Ctx mutant was highly effective as an adjuvant upon i.n. delivery (Yamamoto *et al.*, 1997; Yamamoto *et al.*, 1998), as were non-toxic derivatives of LT (Douce *et al.*, 1997).

When chemically or genetically linked to an antigen (i.e. when employed as a carrier protein), CtxB, but not Ctx, induced oral tolerance (Holmgren *et al.*, 1993; Sun *et al.*, 1994). However, the pentameric B subunit alone may also function as an effective adjuvant to elicit an immune response to co-administered antigens. Studies describing the potency and efficacy of CtxB as an adjuvant have conflicting results. I.n. immunisation in mice against the intestinal nematode *Trichinella spiralis* with a 30-mer peptide antigen and CtxB induced antigen-specific intestinal IgA and serum IgG antibodies (McGuire *et al.*, 2002). Similarly, CtxB was shown to enhance the mucosal antibody response upon oral administration of co-administered influenza (Chen and Strober, 1990). Tochikubo *et al*. (1998) also showed that CtxB increases both mucosal and serum antibody responses to i.n. immunisation with BSA in mice, while, in the same study, these responses were diminished upon oral immunisation. Furthermore, although the i.p. administration of CtxB adjuvant has not been studied to the same extent as that of Ctx, it has been recently shown to enhance both mucosal and serum antibody responses in mice upon i.p. immunisation with BSA (Park *et al.*, 2003). Conversely, CtxB did not significantly increase the antibody response to Japanese cedar

pollen upon i.n. immunisation (Hirai *et al.*, 2000) nor orally-administered keyhole limpet haemocyanin (Lycke and Holmgren, 1986). It was proposed that the adjuvanticity of CtxB may be attributed to the ADP-ribosylase activity from low, contaminating levels of CtxA or holotoxin (Lycke and Holmgren, 1986; Holmgren *et al.*, 1993). However, as noted earlier, toxicologically acceptable variants of Ctx have recently been created whilst retaining adjuvanticity (Pizza *et al.*, 2001; Holmgren and Czerkinsky, 2005). Similarly, while studies with Stx are limited, StxB and an active-site mutant of Stx have also demonstrated adjuvant properties in mice upon i.n. administration with OVA, eliciting both mucosal and systemic antibody responses (Ohmura-Hoshino *et al.*, 2004). Thus, the adjuvanticity of CtxB is an immunological property that is independent of CtxA enzymatic activity.

The ability of Ctx to modulate leukocyte populations has also been studied (Williams *et al.*, 1999; Holmgren *et al.*, 2003). Its effect on antigen presenting cells (APCs) may be the most relevant, as other well-known adjuvants act primarily on APCs (Williams *et al.*, 1999). Indeed, Ctx interaction with APCs, which are critical in priming the immune response, appear to have a significant role in Ctx adjuvanticity as Ctx increases antigen presentation by macrophages, dendritic cells (DCs) and B cells. Indeed, macrophages exposed to Ctx increased secretion of cytokines IL-1, IL-6 and IL-10 (Bromander *et al.*, 1991; Cong *et al.*, 2001) and surface expression of the co-stimulatory molecule, B7.2 (Cong *et al.*, 1997). Furthermore, Ctx has been shown to induce murine and human DC maturation, upregulating expression of HLA-DR, B7.1 and B7.2 molecules and chemokine receptors CXCR4 and CCR7 (Gagliardi *et al.*, 2000; Gagliardi *et al.*, 2002; Eriksson *et al.*, 2003). Although the interactions of CtxB with APCs have not been examined to the extent of those of Ctx, as a carrier molecule, CtxB can increase presentation of co-administered antigen and upregulate CD40 and

B7.2 expression by macrophages and DCs (George-Chandy *et al.*, 2001). Additionally, DCs pre-treated with OVA linked or admixed with Ctx elicited a mixed T_H1 and T_H2 immune response in mice following i.v. injection, whereas CtxB was reported to induce a predominantly T_H2 type response (Eriksson *et al.*, 2003).

1.4 A Novel AB_5 Subtilase Cytotoxin from STEC

Although LEE-positive STEC are the main cause of HUS outbreaks (Nataro and Kaper, 1998; Paton and Paton, 1998), a small outbreak in Adelaide, Australia was caused by LEE-negative O113:H21 STEC expressing Stx2 (Paton *et al.*, 1999). Curiously, the cytotoxicity of the isolate (98NK2) was analogous to that of LEE-positive strains associated with HUS. It was therefore proposed that O113:H21 STEC may express an additional cytotoxin that enhances the severity of Stx2 or induces further pathology. This led to the discovery of the prototype of a novel AB_5 cytotoxin family from 98NK2 (Paton *et al.*, 2004).

Initially, Paton *et al.* (2004) observed that supernatant from 98NK2 possessed residual cytotoxicity on Vero cells despite absorption of all members of the Stx family with a recombinant *E. coli* strain expressing a mimic of the Stx receptor Gb_3, which binds and neutralises Stx with high avidity (Paton *et al.*, 2000b). Similar residual cytotoxicity was observed in supernatant from an *stx*-deleted mutant of 98NK2 constructed by Rogers *et al.* (2003). The toxin operon (GenBank accession number AF399919.3) was located on the 98NK2 megaplasmid pO113 by screening culture supernatants from a 98NK2 cosmid gene bank previously constructed in *E. coli* DH1 (Paton *et al.*, 2001b). The two open reading frames (ORFs) identified, *subA* and *subB*, were shown to be co-transcribed by RT-PCR. The *subA* gene encodes a 347 amino acid secreted protein with greatest homology to the *Bacillus anthracis* gene product BA_2875 (26% identity and 39% similarity over 246 amino acids). Similarities to the

serine protease family of Peptidate_S8 subtilases (pfam00082.8) were also noted while PROSITE analysis indicated the presence of three conserved sequence domains comprising the catalytic triad (separate domains of ~11 amino acids located around residues Asp52, His89 and Ser272), which is characteristic of the subtilase family (Siezen *et al.*, 1991). The 141 amino acid protein encoded by *subB* displayed similarities to putative exported proteins from *Salmonella* Typhi, STY1891 (50% identity and 68% similarity over 117 amino acids) and *Yersinia pestis*, YPO0337 (56% identity and 79% similarity over 136 amino acids).

The *subAB* operon was present in 32 out of 68 other STEC strains tested by PCR or Southern hybridisation including serogroups O23, O48, O82, O91, O111, O113, O123, O128, O157, OX3 and O non-typable strains (Paton *et al.*, 2004), which provides a possible explanation for the cytotoxicity of strains that apparently do not harbour genes encoding Stx. However, the genes were not located in the two published genome sequences of STEC O157:H7 (Hayashi *et al.*, 2001; Perna *et al.*, 2001). Furthermore, a strong correlation between the presence of *subA* and *stx2*, but not *stx1* in STEC was established (Paton and Paton, 2005).

1.4.1 SubAB Structure and Function

Densitometry analysis of Coomassie blue-stained SDS-PAGE gels of purified SubAB cytotoxin indicated that the 35-kDa SubA and 14-kDa SubB proteins were present in an approximate 1:5 molar ratio. Furthermore, subjecting purified SubAB to mild cross-linking conditions before SDS-PAGE analysis revealed that the holotoxin has a molecular size of approximately 105 kDa. Hence, this indicated that SubA and SubB form a stable AB_5 complex under non-denaturing conditions. The two open reading frames of *subA* and *subB* were cloned into plasmid pK184 and transformed into *E. coli* JM109. Site-directed mutagenesis of the critical SubA active site residue, Ser272

reduced supernatant and cell lysate cytotoxicity by more than 99.9%. Therefore, SubA has a serine protease activity that is central to the mechanism of action of the holotoxin. Interestingly, while micro-organisms commonly employ subtilase-like serine proteases as extracellular enzymes for defence or growth on proteinaceous substrates, none have been shown to be cytotoxic (Siezen *et al.*, 1991; Siezen and Leunissen, 1997). Furthermore, the enzymatic activity of SubAB is distinct from all other AB_5 toxins currently known (Stx is an RNA *N*-glycosidase, while Ctx, LT and Ptx are ADP-ribosyltransferases). Accordingly, the new toxin was named "subtilase cytotoxin" (Paton *et al.*, 2004).

SubAB is 10 – 100 times more toxic for Vero cells than Stx *in vitro* (Paton *et al.*, 2004). Its extreme cytotoxicity for eukaryotic cells was shown to be due to a specific single-site cleavage of BiP (also known as GRP78) (Paton *et al.*, 2006a). BiP is an ER-resident chaperone of the Hsp70 family comprising an amino-terminal ATPase and a C-terminal protein-binding domain. It facilitates correct folding of nascent secretory proteins and seals the lumenal end of the Sec61 translocon pore to maintain the permeability barrier of the ER membrane, as well as directing terminally mis-folded proteins to the Sec61 apparatus for degradation by the proteasome (Gething, 1999; Hendershot, 2004). BiP plays a crucial role in the unfolded protein response as the master regulator of ER stress-signalling and demonstrates anti-apoptotic properties by inhibiting caspase activation (Kim and Arvan, 1998; Rao *et al.*, 2004). SubAB cleaves a di-leucine motif in the hinge connecting the ATPase and protein-binding domains of BiP (Paton *et al.*, 2006a), and the loss of BiP function has inexorably fatal consequences for the cell (Hamman *et al.*, 1998; Kim and Arvan, 1998; Rao *et al.*, 2004; Lee, 2005). Similar to the effects of Stx, SubAB was shown to transiently inhibit protein synthesis

for up to 2 h in Vero cells (Morinaga *et al.*, 2007; Morinaga *et al.*, 2008), which is most likely an indirect consequence of BiP cleavage.

SubAB is highly specific for a subtilase-like serine protease, and does not appear to cleave any other host cell protein, including the most closely-related chaperones Hsp70 and Hsc70. The crystal structure of SubA revealed that this extraordinary specificity may be due to its catalytic site being partially occluded and residing at the bottom of a deep cleft (Paton *et al.*, 2006a). SubAB is the first cytotoxin that has been shown to target a eukaryotic chaperone protein or a component of the ER and is the only AB toxin whose specific substrate is not located in the cytosolic compartment. Consequently, the activity of SubAB has been employed as a tool in cell biology to induce ER stress and the unfolded protein response (Takano *et al.*, 2007; Buchkovich *et al.*, 2008; Hayakawa *et al.*, 2008).

1.4.2 Sialic Acid as a Putative Receptor

Similar to other bacterial AB_5 toxins, the SubB pentamer facilitates recognition of a previously-uncharacterised host cell oligosaccharide and there is strong evidence to suggest that the glycan receptor is of an acidic nature, containing at least one sialic acid residue (Paton *et al.*, 2004; Yahiro *et al.*, 2006). As distal glycan residues of cell surface glycoconjugates, sialic acids facilitate lectin-mediated intercellular signalling, as well as host recognition by microbial toxins (Svennerholm, 1980; Muchmore *et al.*, 1998). Variations of the most prevalent sialic acid, N-acetylneuraminic acid (Neu5Ac), can alter these endogenous and exogenous interactions (Troy, 1992; Varki, 1992; Ye *et al.*, 1994; Kelm and Schauer, 1997).

Toxin extracts were absorbed with recombinant *E. coli* strains expressing receptor mimic constructs (RMCs) of the glycan domains of Gb_3, Gb_4 and monosialo-GGS GM_2 after which, the residual Vero cytotoxicity was measured (Paton *et al.*,

2004). Despite no discernable reduction of cytotoxicity observed by absorption with Gb_3 and Gb_4 RMCs, SubAB activity was neutralised by 93.4% when absorbed with the GM_2 RMC. Vero cell membrane GGS extracts were also analysed by TLC for the presence of GM_2 in the same study. Orcinol reagent detection indicated that extracts harboured a species with a similar mobility to that of a commercial GM_2 standard. Since previous bacterial RMCs have neutralised their cognate toxins with an efficacy in excess of 98% (Paton *et al.*, 2000b; Paton *et al.*, 2001a), this suggests that although SubAB may bind GM_2, the toxin potentially has a greater affinity for a variant of this acidic oligosaccharide structure. Furthermore, Yahiro *et al*. (2006) reported that SubB can bind α2β1 integrin (a sialylated glycoprotein (Bellis, 2004)). However, association with this receptor was only shown to cause vacuolation of Vero cells using high concentrations (greater than 1 $\mu g.ml^{-1}$) of either SubAB or SubB, but not SubA (Yahiro *et al.*, 2006; Morinaga *et al.*, 2007). As host cell vacuolation is independent of SubA serine protease activity, α2β1 is unlikely to be a functional receptor for SubAB-mediated BiP cleavage.

1.4.3 Aetiology of Disease

In vivo toxicity of SubAB was studied by i.p. injection of mice with purified toxin (Paton *et al.*, 2004); all mice died and survival times were inversely related to their SubAB dose from 2 days at 25 μg to 8 – 10 days with 200 ng. In the murine model, death was preceded by ataxia and hind limb paralysis suggesting neurological damage and histology sections exhibited extensive microvascular thrombosis and necrosis in the kidneys, liver and brain. Groups of mice that were fed an *E. coli* clone expressing SubAB, DH5α:pK184*subAB* (maintaining 10^8 – 10^9 $cfu.g^{-1}$ faeces throughout the experiment) appeared ill and lethargic and had lost up to 15.7% of their mean starting weight after six days treatment. However, the challenged mice steadily

gained weight from day seven, which was attributed to seroconversion. In contrast, the weight gain of mice that were fed the negative control DH5α:pK184 was statistically indistinguishable from those with the DH5α:pK184*SubA*$_{A272}$*B* expressing the inactive SubAB mutant. This demonstrated that enteric delivery of SubAB was directly responsible for the detrimental effects on the animals.

Further *in vivo* studies have shown that mice injected with 5 µg SubAB i.p. develop pathological features that overlap those of animals injected with Stx and STEC-associated HUS in humans (Wang *et al.*, 2007). Within 24 h of treatment with SubAB, mice exhibited renal damage, characterised by a statistically significant increase in blood urea content and proteinuria. There was also no evidence of glucosuria, which is contrary to studies with Stx in mice that develop glucosuria, but not proteinuria (Rutjes *et al.*, 2002). Neutrophil infiltration was observed in the kidneys, liver and spleen at 24 h, but not the brain or ileum. Furthermore, increased apoptosis of hepatocytes and splenic lymphocytes and neutrophils was apparent at 24 h while renal tubule apoptosis was observed at 48 h. Elevated aspartate aminotransferase and creatine phosphokinase (CPK) levels in the blood 48 h after injection were indicative of impaired liver function and myocardiopathy, respectively, while increased blood lactate dehydrogenase levels suggest a generalised toxicity such as haemolysis. Indeed, 24 h after injection, blood smears demonstrated substantial erythrocyte fragmentation (indirectly caused by microangiopathy), decreased platelet counts and leukocyte apoptosis or necrosis.

Despite SubAB treatment elevating blood CPK levels, histological examination did not reveal any obvious cardiac damage. Extensive damage, however, was observed in the kidneys, liver, spleen and brain. By 24 h SubAB treatment caused renal cortical haemorrhaging, congested glomeruli and hepatocytes exhibited haemorrhagic foci and reduced sinusoidal spaces. Splenic leukocytes had infiltrated the red pulp, while the

cerebrum, cerebellum and brain stem exhibited microvascular thrombosis. By 72 h, thrombi were more pervasive, glomeruli showed signs of microthrombotic angiopathy and necrotic thrombosis and the liver had developed haemorrhagic foci. Furthermore, the spleen had diminished to approximately one third its normal size indicating necrosis and the cerebellum and brain stem had developed haemorrhagic foci which are thought to be the cause of ataxia and sudden death observed 3 to 4 days after SubAB exposure.

Despite the pathological similarities between those elicited by SubAB and Stx, SubAB also causes several distinct symptoms that have not been attributed to Stx. In addition to proteinuria highlighted earlier, SubAB treatment elevated liver enzyme levels in the blood and caused significant liver damage including microthrombi, decreased sinusoidal spaces and haemorrhagic and necrotic foci. Furthermore, the toxin induced marked splenic atrophy, neutrophil infiltration and leukocyte redistribution. The production of two potentially lethal cytotoxins by a single pathogen raises interesting questions about the relative importance of each toxin to human disease pathogenesis, and whether they might act in synergism. While the origin of this new family of AB_5 subtilase cytotoxins is uncertain, it represents the outcome of two ostensibly benign genetic elements such as *subA* and *subB* that are brought into close proximity to one another.

1.5 Hypothesis and Aims

The recently-discovered AB_5 subtilase cytotoxin released by STEC is a potent novel virulence factor that has the potential to contribute significantly to morbidity and mortality in humans. Montecucco *et al.* (1994) outlined a general four-step mechanism by which bacterial protein toxins can infiltrate eukaryotic cells, characterised by a distinct topological presentation of the toxin with respect to the target cell. Briefly, it is supposed that the toxin binds to the cell surface via its B subunit, which is followed by endocytosis and intracellular trafficking of the toxin. The catalytic A subunit subsequently escapes the membrane-bound vesicle and consequently exerts its enzymatic activity toward a specific intracellular target. As the intracellular substrate of SubAB has been identified as the ER chaperone BiP (Paton *et al.*, 2006a), the research to be undertaken will investigate the initial steps by which SubAB permeates the eukaryotic target cell to address a fundamental gap in our understanding of the mechanisms of cytotoxicity of a novel STEC virulence factor. Given the previous characterisation of Ctx and Stx, it is proposed that SubAB binds to a membrane-bound glycolipid receptor, is actively taken up by the host cell and trafficked through the cell to its ER target BiP by a mechanism such as retrograde transport. It is also anticipated that SubB possesses immunomodulating properties and may be employed as a systemic adjuvant similar to those of CtxB and StxB. Accordingly, the aims of the work described in this thesis are:

1. To identify the carbohydrate structure on the host cell surface recognised by SubAB;
2. To determine the intracellular trafficking pathway of SubAB;
3. To assess the capacity for SubB to enhance the host immune response toward a co-administered antigen and compare its activity to that of other adjuvants.

CHAPTER 2
MATERIALS AND METHODS

2.1 Chemicals, Reagents and Enzymes

Most chemicals used were AnalaR grade and were purchased from Ajax Chemicals (NSW, Australia). Tris was purchased from Amresco Inc. (Solon, OH). Acrylamide was purchased from Bio-Rad Laboratories (Hercules, CA). Isopropyl-β-D-thiogalactoside (IPTG) and was purchased from Roche Diagnostics GmbH (Mannheim, Germany). Polyisobutylmethacrylate (PIBM) was purchased from Aldrich Chemical Company (Milwaukee, WI). Ammonium persulphate (APS), N,N,N'N'-tetramethyl-ethylene-diamine (TEMED), brefeldin A (BFA), 5-bromo-2'-deoxyuridine (BrdU), chlorpromazine (CPZ), filipin, genistein, MβCD, nocodazole and phenylarsine oxide (PAO) were purchased from Sigma Chemical Company (St. Louis, MO).

2.1.1 Antibiotics

Ampicillin (Amp) was purchased from Commonwealth Serum Laboratories Ltd. (Vic, Australia). Kanamycin sulphate (Kan) was purchased from Progen Industries (QLD, Australia).

2.1.2 Tissue Culture Media and Reagents

Dulbecco's Modified Eagle Medium (DMEM) (Dulbecco and Freeman, 1959), Eagle's Minimum Essential Medium (MEM) with Earle's balanced salt solution, RPMI 1640, viral production serum-free medium (VP-SFM), foetal calf serum (FCS), L-glutamine, penicillin-streptomycin (Pen-Strep) and trypsin-EDTA were purchased from Invitrogen (VIC, Australia). Trypan blue was purchased from Merck (VIC, Australia). Dimethyl sulfoxide (DMSO) was purchased from Sigma.

2.2 Plasmids, Bacterial Strains and Cell Lines

Plasmids, bacterial strains and cell lines used in this study are listed in Table 2.1, Table 2.2 and Table 2.3, respectively.

Table 2.1: Plasmids used in this study.

Plasmid	Description	Source (reference)
pCaveolin-1-EGFP	Dark Agoutic rat Caveolin-1 in pEGFP-N1	(Eyre *et al.*, 2006)
pCst	*Campylobacter jejuni cstII* in pUC21	(Paton *et al.*, 2005)
pEGFP-N1	f1 ori; pUC ori; SV40 ori; $P_{CMV\ EI}$; *egfp*; Kan^R/Neo^R (GenBank #: U55762)	Clontech Laboratories, Inc, Palo Alto, CA
pJCP-$_{Gb3}$	Kan^R; *Neisseria lgtC* and *lgtE* in pK184	(Paton *et al.*, 2000b)
pJCP-Gb_4	Kan^R; *Neisseria lgtD* and *E. coli* O113 *gne* in pJCP-Gb_3	(Paton *et al.*, 2001a)
pJCP-GM_1	Kan^R; *C. jejuni cgtA* and *cgtB*, *Neisseria lgtE*, and *E. coli* O113 *gne* in pK184	(Focareta *et al.*, 2006)
pJCP-GM_2	Kan^R; *C. jejuni cgtA*, *Neisseria lgtE*, and *E. coli* O113 *gne* in pK184	(Paton *et al.*, 2005)
pJCP-GM_3	Kan^R; *Neisseria lgtE*, and *E. coli* O113 *gne* in pK184	Paton, A. W., University of Adelaide, Australia
pJCP-LgtE	Kan^R; *Neisseria lgtE* in pK184	(Paton *et al.*, 2000a)
pK184	ColE1 compatibility; p15a ori; *lacZ*α; Kan^R (GenBank #: U000800)	(Jobling and Holmes, 1990)
pUC21	pUC ori; *lacZ*α; Amp^R (GenBank #: AF223641)	(Vieira and Messing, 1991)

Table 2.2: Bacterial strains used in this study.

***E. coli* strain**	**Description**	**Source (reference)**
CWG308	Gen^R *waaO*::*aacC1* derivative of *E. coli* F470 (R1 core; R-LPS derivative of *E. coli* O8:K27)	(Heinrichs *et al.*, 1998)
CWG308:pJCP-Gb_3	CWG308 transformed with pJCP-Gb_3	(Paton *et al.*, 2000b)
CWG308:pJCP-Gb_4	CWG308 transformed with pJCP-Gb_4	(Paton *et al.*, 2001a)
CWG308:pJCP-GM_1	CWG308 transformed with pJCP-GM_1 and pCst	(Focareta *et al.*, 2006)
CWG308:pJCP-GM_2	CWG308 transformed with pJCP-GM_2 and pCst	(Paton *et al.*, 2005)
CWG308:pJCP-GM_3	CWG308 transformed with pJCP-GM_3 and pCst	Paton, A. W., University of Adelaide
CWG308:pJCP-LgtE	CWG308 transformed with pJCP-LgtE	(Paton *et al.*, 2000b)

Table 2.3: Cell lines used in this study.

Cell line	**Description**	**Source**
HCT-8	Human colonic epithelial; colorectal adenocarcinoma (ATCC#: CCL-244)	Division of Veterinary and Biomedical Sciences, Murdoch University, Murdoch, WA, Australia
HeLa	Human cervical epithelial; adenocarcinoma (ATCC #: CCL-21)	University of Adelaide, Adelaide
N2A	Mouse (*Mus musculus*) brain neuroblastoma (ATCC#: CCL-131)	Institute of Medical and Veterinary Science, Adelaide, SA, Australia
Vero	African Green Monkey (*Cercopithecus aethiops*) kidney epithelial (ATCC #: CCL-81)	Institute of Medical and Veterinary Science, Adelaide, SA, Australia

2.3 Carbohydrate Structures

The carbohydrate structures used in this study are listed in Table 2.4.

Table 2.4: Receptor analogues used in this study[a].

Receptor	Oligosaccharide Structure or Description	Source (reference)
α_1-AGP	Sialylated glycoprotein from human or ovine plasma	Sigma
Chen-1	Neu5Acα(2→3)LacβProN_3	CFG Core D, CA
Chen-2	Neu5Gcα(2→3)LacβProN_3	CFG Core D
Chen-3	Neu5Acα(2→3)LacNAcβProN_3	CFG Core D
Chen-4	Neu5Gcα(2→3)LacNAcβProN_3	CFG Core D
Chen-5	Neu5Acα(2→3)Galβ(1→3)GlcNAcβProN_3	CFG Core D
Chen-6	Neu5Gcα(2→3)Galβ(1→3)GlcNAcβProN_3	CFG Core D
Gb_3	Galα(1→4)Galβ	See Table 2.2
Gb_4	GalNAcβ(1→3)Galα(1→4)Galβ	Sigma See also Table 2.2
GM_1	Neu5Acα(2→3) [Galβ(1→3)GalNAcβ(1→4)]Galβ(1→4)Glcβ	Sigma See also Table 2.2
aGM_1	Galβ(1→3)GalNAcβ(1→4)Galβ(1→4)Glcβ	Sigma
GM_2	Neu5Acα(2→3)[GalNAcβ(1→4)]Galβ(1→4)Glcβ	Sigma See also Table 2.2
GM_3	Neu5Acα(2→3)Galβ(1→4)Glcβ	Sigma See also Table 2.2
GD_{1a}	Neu5Acα(2→3)[Neu5Acα(2→3) Galβ(1→3)GalNAcβ(1→4)]Galβ(1→4)Glcβ	Sigma
GD_{1b}	Neu5Acα(2→8)Neu5Acα(2→3) [Galβ(1→3)GalNAcβ(1→4)]Galβ(1→4)Glcβ	Sigma
LgtE	Galβ	See Table 2.2
Neu5Gc	Neu5Gc	Sigma

[a] Adapted from Sigma catalogue and the Consortium for Functional Glycomics (CFG) Core D carbohydrate database.

2.4 Bacterial Growth Media

E. coli strains were grown in Luria-Bertani (LB) broth (10 $g.L^{-1}$ tryptone-peptone [Difco, MD], 5 $g.L^{-1}$ Bacto yeast extract [Difco], 5 $g.L^{-1}$ NaCl, pH 7.5), Terrific broth (24 $g.L^{-1}$ yeast extract, 12 $g.L^{-1}$ tryptone-peptone, 0.4% [v/v] glycerol, 0.17 M KH_2PO_4, 0.72 M K_2HPO_4) or on LB agar plates (LB with 1.5% [w/v] Bacto agar [Difco]). Where appropriate, Amp and Kan was added to the growth medium at concentrations of 100 $\mu g.ml^{-1}$ and 50 $\mu g.ml^{-1}$, respectively. When grown in LB, bacteria were incubated at 37°C with aeration; when grown on LB agar, bacteria were incubated at 37°C statically. *E. coli* strains were preserved in LB broth supplemented with 30% (v/v) glycerol at –80°C.

2.5 SubAB Expression and Purification

2.5.1 SubAB Expression

SubAB and $SubA_{A272}B$ were expressed and purified essentially as described by Paton *et al.* (2004) and Talbot *et al.* (2005).

Expression strains were grown in 500 ml Terrific broth supplemented with 50 $\mu g.ml^{-1}$ Amp at 37°C with agitation overnight. The following day, 1 L of Terrific broth was added with antibiotics and 5 mM IPTG and incubated at 37°C with agitation for 3 h. The culture was then centrifuged at 4°C for 10 min at 12,000 × *g* and the supernatant removed. The pellet was resuspended in 20 ml of loading buffer (50 mM sodium phosphate, 300 mM NaCl, pH 8.0), and the cells were lysed using an Aminco French pressure cell (SLM Instruments, Urbana, IL) operated at 12,000 psi. Cell debris was subsequently removed by centrifugation at 4°C for 1 h at 100,000 × *g*.

2.5.2 Affinity Purification

The supernatant from Section 2.5.1 was then loaded onto a 4-ml column of ProBond Ni-nitrilotriacetic acid resin (Invitrogen, Carlsbad, CA) after pre-equilibrating with 10 ml loading buffer. The column was subsequently washed with 15 ml wash buffer (50 mM sodium phosphate, 300 mM NaCl, 10% glycerol, pH 6.0). Bound proteins were eluted with a 30-ml gradient of 0 – 500 mM imidazole in wash buffer and 3-ml fractions were collected and analysed by SDS-PAGE (Section 2.6.1). Peak fractions were pooled, diafiltered against PBS and stored in 50% glycerol at –20°C.

2.6 General SDS-PAGE

2.6.1 SDS-PAGE

SDS-PAGE was carried out as described by Laemmli (1970). Samples were boiled for 5 min, loaded on acrylamide gels and subjected to electrophoresis in a Hoefer Mighty Small II SE250 gel apparatus (Amersham Biosciences, Piscataway, NJ) at 170 V for 1 h 45 min. Separating gels comprised 16% (v/v) acrylamide, 142 mM Tris (pH 8.8), 0.05% (w/v) SDS, 0.04% (v/v) APS and 0.014% (v/v) TEMED while the stacking gels comprised 3% (v/v) acrylamide, 62 mM Tris (pH 6.8), 0.05% (w/v) SDS, 0.04% (v/v) APS and 0.11% (w/v) TEMED. BenchMark pre-stained protein ladder (Invitrogen) was used as an SDS-PAGE marker with sizes of 172, 110.2, 79, 62.4, 48, 36.6, 24.5, 19, 13.5 and 5.3 kDa.

2.6.2 Western Transfer (Nitrocellulose)

The method used was an adaptation of that described by Towbin *et al.* (1979) in which samples run on gels from Section 2.6.1 were transferred onto a nitrocellulose membrane (BioTrace NT, Pall Corporation, MI) at 300 mA for 1 h in transfer buffer (25

mM Tris [pH 8.3], 192 mM glycine, 10% [v/v] methanol) using a Hoefer Transphor electrophoresis unit TE223 (Amersham Biosciences).

2.6.3 Western Blot Analysis

Membrane sheets from Section 2.6.2 were blocked by incubating in 5% (w/v) skim milk powder in Tween-Tris-buffered saline (TTBS; 0.5% [v/v] Tween-20, 200 mM Tris, 9% [w/v] NaCl, pH 7.4) for 1 h with gentle shaking. Blocking solution was decanted and the membrane incubated in goat anti-BiP (C-20; Santa Cruz) diluted 1:5,000 in TTBS at room temperature overnight with gentle shaking. The serum was removed and the nitrocellulose filter was washed three times for 10 min with TTBS with gentle shaking. The membrane was then incubated in rabbit anti-goat-AP (BioRad Laboratories, CA) diluted 1:5,000 in TTBS containing 0.02% (w/v) skim milk powder for 1 h with gentle shaking. After washing with TTBS as before, filters were developed as described in Section 2.10.5.

2.6.4 Pre-Cast SDS-PAGE

Samples were loaded into 12% pre-cast NuPAGE Bis-Tris gels (Invitrogen) and subjected to electrophoresis in an Xcell SureLock electrophoresis cell (Invitrogen) at 200 V for 55 min. The cell contained either NuPAGE MES or LDS SDS running buffer for reducing or non-reducing conditions, respectively. Gels were removed from plastic casings and either silver stained (Section 2.6.5) or transferred onto a polyvinylidene difluoride (PVDF) membrane (Section 2.6.6).

2.6.5 Silver Staining of SDS-PAGE Gels

Pre-cast gels were incubated in fixing solution (40% [v/v] ethanol, 5% [v/v] glacial acetic acid) for 1 h with gentle shaking. The fixing solution was decanted and replaced with oxidising solution (40% [v/v] ethanol, 5% [v/v] glacial acetic acid, 0.7%

periodic acid) for 5 min with shaking. After removing the oxidising solution and three 10 min washes with MQ H_2O, gels were stained with staining solution (50 mM NaOH, 1.3% [v/v], NH_4OH, 3.3% [v/v] $AgNO_3$) for 10 min with shaking and washed with MQ H_2O as before. Gels were developed in 0.01% (w/v) citric acid, 3.7% (v/v) formaldehyde and stopped by incubating in 4% (v/v) acetic acid for 15 min with shaking.

2.6.6 Western Transfer (PVDF)

Before use, PVDF membranes were soaked in methanol, rinsed in MQ H_2O then equilibrated in 1 × transfer buffer (Invitrogen) containing 20% (v/v) methanol. Samples electrophoresed in pre-cast gels from Section 2.6.4 were transferred onto a PVDF membrane (BioTrace NT, Pall Corporation, MI) in an XCell SureLock apparatus (Invitrogen), as described by the manufacturer, at 30 V for 1 h.

2.7 Tissue Culture Growth Media

DMEM when purchased (Invitrogen) contained additives of 4.5 $g.L^{-1}$ glucose with sodium pyruvate, 20 mM HEPES and L-glutamine, MEM contained Earle's balanced salt solution and non-essential amino acids, and RPMI 1640 contained L-glutamine. DMEM, MEM and RPMI 1640 were supplemented with Pen-Strep (100 $U.ml^{-1}$ penicillin G sodium, 100 $\mu g.ml^{-1}$ streptomycin sulfate in 0.85% saline) used at 1% (v/v). L-glutamine (200 mM) was added to DMEM, MEM, RPMI 1640 and VP-SFM every fortnight at 1% (v/v). Media were stored at 4°C until required. MEM was supplemented with 1.5 $g.L^{-1}$ sodium bicarbonate and 1 mM sodium pyruvate.

Vero cells were grown in DMEM with 5% FCS, Pen-Strep and L-glutamine or VP-SFM with L-glutamine. HCT-8 cells were grown in RPMI 1640 with 5% FCS, Pen-

Strep and L-glutamine. HeLa cells were grown in MEM with 5% FCS, Pen-Strep and L-glutamine.

2.8 Tissue Culture Techniques

2.8.1 Retrieval of Cells from Cryostorage

Cryovials containing cells were rapidly thawed in a 37°C water bath and washed in 10 ml DMEM or RPMI 1640 by centrifugation at 400 × *g* for 10 min. Cells were resuspended in 20 ml of the appropriate growth medium, transferred into a ventilated 75-cm^2 flask (BD Falcon, Franklin Lakes, NJ) and grown at 37°C in a humidified 95% (v/v) air/5% (v/v) CO_2 atmosphere.

2.8.2 Propagation

Cells that had grown to 90% confluence were washed twice with phosphate-buffered saline (PBS; 0.137 M NaCl, 2.7 mM KCl, 8.1 mM Na_2HPO4, 1.5 mM KH_2PO_4, pH 7.4) and incubated with 1 ml trypsin-EDTA (0.25% (w/v) trypsin, 0.02% (w/v) EDTA in PBS) until the cells began to detach. Cells were suspended in 10 ml of the appropriate medium and split 1:5 twice a week.

2.8.3 Cryostorage

Trypsinised cells (described above) were suspended in 10 ml of the appropriate medium, pelleted at 400 × *g*, resuspended in 2 ml freezing solution (70% [v/v] DMEM or RPMI 1640, 20% [v/v] FCS, 10% [v/v] DMSO) and stored at –80°C or in liquid nitrogen.

2.8.4 Transfection of Cells with pCaveolin-1-EGFP

Six-well trays were seeded with 1 ml of Vero cell suspension harvested in Section 2.8.2, made up to 2.5 ml with growth medium and grown to 50 – 75%

confluence at 37°C overnight. Cells were transfected with pCaveolin-1-EGFP using either FuGENE 6 Transfection Reagent (Roche) or Lipofectamine 2,000 (Invitrogen) according to the manufacturers' instructions.

Transfectants were confirmed by fluorescence microscopy, as detailed in Section 2.16.1. Cells were trypsinised and pooled into a 75-cm^2 flask with transfectants selected by incubating in growth medium supplemented with 800 $\mu g.ml^{-1}$ geneticin (G418) (Invitrogen), replacing the media every two days for two weeks. GFP-expressing transfectants were sorted with the assistance of Sandy Macintyre (Institute of Medical and Veterinary Science, Adelaide, SA) using a BD FACSAria (BD Biosciences, San Jose, CA) with FACSDiva Software v4.1.2 and maintained in growth medium containing 250 $\mu g.ml^{-1}$ G418.

2.9 Cytotoxicity Assay

2.9.1 Determining the Specific Cytotoxicity of SubAB

Vero cells were seeded into 96-well flat-bottom trays (BD Falcon) and incubated overnight at 37°C until confluent. Confluent monolayers were washed twice with PBS, treated with 100 µl of toxin that had been serially diluted 10-fold in DMEM without FCS, and incubated at 37°C for 30 min. After incubation, 100 µl of medium supplemented with 2% FCS was added per well and cytotoxicity was assessed microscopically after four days of incubation at 37°C. The toxin CD_{50} was defined as the reciprocal of the maximum dilution producing a cytopathic effect on at least 50% of the cells in each well.

2.9.2 Receptor Analogue Toxin Inhibition

The glycan moieties of α_1-Acid glycoprotein (α_1-AGP) derived from human and sheep plasma, synthetic trisaccharides Chen-1 to Chen-6 (structures presented in Table

2.4) and commercially available N-glycolylneuraminic acid (Neu5Gc) were assessed for their capacity to reduce the specific cytotoxicity of SubAB. Initially, Vero cells were seeded overnight in a 96-well microtitre tray as described in Section 2.9.1. 0.1 $\mu g.ml^{-1}$ SubAB in DMEM with 2% FCS was incubated at 37°C for 30 min with 10-fold serial dilutions of these sialylated compounds, beginning with a 100:1 glycan:toxin mass ratio (1000:1 when using α_1-AGP), where the molecular weight of α_1-AGP was assumed to be 40.8 kDa as demonstrated by sedimentation velocity and diffusion studies (Charlwood *et al.*, 1976). Vero cells were then exposed to 100 µl of the glycan-SubAB solution and cytotoxicity was assessed microscopically after four days of incubation at 37°C.

2.10 Eukaryotic Glycolipid Receptors

2.10.1 Ganglioside and Neutral Glycosphingolipid Separation

Trypsinised eukaryotic cells (described in Section 2.8.2) were harvested in 10 ml of the appropriate medium, pelleted at 400 × *g*, resuspended in a minimal volume of MQ H_2O and stored at –20°C until required. Gangliosides (GGSs) and neutral glycosphingolipids (GSLs) were extracted from mammalian cell membranes essentially as described by Folch, *et al*. (1951) adapted with the assistance of Peter Sharp (Chemical Pathology Department, Women's and Children's Hospital, North Adelaide, SA, Australia) where 1 g tissue was assumed to be equivalent to 1 ml aqueous cell suspension. Cell pellets were rapidly thawed in a 37°C water bath and ruptured by ultra-sonication for 40 s on ice. Twenty volumes of chloroform:methanol (2:1) were added to the sample and allowed to stand at room temperature for at least 1 h. Samples were partitioned by adding 0.2 volumes 0.1 M KCl, allowed to stand at room temperature for 15 min, then centrifuged at 1,500 × *g* for 5 min.

2.10.2 Reverse Phase Ganglioside Extraction

A 100 mg C18 solid phase extraction cartridge (United Chemical Technologies, Bristol, PA) was primed with five column volumes of methanol and washed with five column volumes of MQ H_2O. The upper phase from centrifugation in Section 2.10.1 was applied to the cartridge under gravity and washed with 10 column volumes of MQ H_2O. GGSs were subsequently eluted with 10 column volumes of methanol, dried at 37°C under nitrogen, resuspended in chloroform:methanol (2:1) and stored at –20°C.

2.10.3 Normal Phase Neutral Glycosphingolipid Extraction

A 100 mg silica solid phase extraction cartridge (United Chemical Technologies) was primed with two column volumes of acetone:methanol (9:1) and washed with two column volumes of chloroform. The lower phase from centrifugation in Section 2.10.1 was applied to the cartridge under gravity and washed with 10 column volumes of chloroform. GSLs were subsequently eluted with ten column volumes of methanol, dried at 37°C under nitrogen, resuspended in chloroform:methanol (2:1) and stored at –20°C.

2.10.4 Thin-Layer Chromatography

Approximately 25 µl of GGS and neutral GSL extracts from Section 2.10 were loaded in replicate 1 cm-wide tracks on an aluminium-backed 0.2 mm Nano Silica gel 60 high-performance TLC plate (Alltech Associates, Baulkham Hills, NSW, Australia) and allowed to dry at room temperature. Approximately 5 µg of the GGS standards asialo-ganglioside 1 (aGM_1), monosialo-gangliosides 1, 2 and 3 (GM_1, GM_2 and GM_3, respectively) and disialo-gangliosides 1a and 1b (GD_{1a} and GD_{1b}, respectively) and the GSL standard globotetraosyl ceramide (Gb_4) were also loaded in adjacent replicate tracks. GGSs were separated by developing plates in chloroform:methanol:0.2% (w/v)

$CaCl_2$ (60:35:8 [v/v/v]) in a closed glass TLC tank (Alltech), while GSLs were separated using chloroform:methanol:MQ H_2O (65:25:4 [v/v/v]). Replicate tracks of GGS and GSL membrane extracts to be used in Section 2.10.5 were cut off while total glycolipid composition was visualised by spraying with 2 $mg.ml^{-1}$ orcinol monohydrate (Sigma) in 75% (v/v) H_2SO_4 and baking the chromatogram at 125°C for 10 min.

2.10.5 Toxin Overlay Assay (Glycolipids)

Glycolipid specificities of toxins were determined by an amalgamation of the procedures described by Magnani *et al.* (1980), Lingwood *et al.* (2000) and Suetake and Yu (2003). The duplicate tracks cut off in Section 2.10.4 were saturated in *n*-hexane:chloroform (9:1) containing 0.2% (w/v) PIBM using a Preval sprayer (Alltech), allowed to air dry, and blocked overnight with 5% (v/v) FCS in Tris-buffered saline (TBS; 200 mM Tris, 9% [w/v] NaCl, pH 7.4) at 4°C or with 1% (w/v) gelatin in TBS at 37°C. TLC plates were rinsed in TBS then washed three times for 10 min in TBS at room temperature with gentle shaking, and overlaid with or without 1 $\mu g.ml^{-1}$ SubAB or 0.5 $\mu g.ml^{-1}$ CtxB conjugated to peroxidase (CtxB-POD) (Sigma) in the blocking solution and allowed to stand at 4°C overnight.

Plates exposed to toxin were rinsed and washed as before and incubated in mouse anti-His_6 mAb (Qiagen), diluted 1:3,000 in the blocking solution at 4°C overnight. Plates were then washed and incubated in goat anti-mouse IgG conjugated to alkaline phosphatase (AP) (BioRad) diluted 1:6,000 in the blocking solution at 4°C overnight. Plates were washed, equilibrated in digoxigenin (DIG) buffer 3 (100 mM Tris-HCl, 100 mM NaCl, 50 mM $MgCl_2$, pH 9.5) for 5 min, drained and developed in 10 ml DIG 3 containing 45 µl DIG 4 (75 $mg.ml^{-1}$ nitroblue [tetrazolium salt] in 70% [v/v] dimethyl formamide) and 35 µl DIG 5 (50 $mg.ml^{-1}$ 5-bromo-4-chloro-indolylphosphate [toluidinium salt] in dimethyl formamide). Once sufficient colour had

developed, the reaction was stopped by soaking in Tris-EDTA (TE; 10 mM Tris, 1 mM EDTA, pH 8.0) for at least 30 min.

Plates incubated with CtxB-POD were rinsed, washed as before and developed in 9.9 ml methanol containing 3 $mg.ml^{-1}$ 4-chloro-1-naphthol freshly mixed with 16.5 ml TBS and 1:1,000 dilution of 30% H_2O_2. When sufficient colour had developed, the reaction was stopped with extensive washing under tap water.

2.11 Eukaryotic Glycoprotein Receptors

2.11.1 Glycoprotein Receptor Isolation

Immunoprecipitation of putative receptor proteins was performed as described by Yahiro *et al.* (2006) in which 5×10^7 Vero cells were detached with TNE buffer (40 mM Tris [pH 7.5], 150 mM NaCl, 1 mM EDTA) then washed twice with PBS. Cell surface proteins were biotinylated using EZ-Link Sulfo-NHS-Biotin (Pierce Biotechnology, Rockford, IL) according to the manufacturer's instructions. Cells were lysed with 1 ml Sol buffer (50 mM Tris [pH 7.5], 100 mM NaCl, 10% [v/v] glycerol, 1% [v/v] Triton X-100) and 50 µl protease inhibitor cocktail (Sigma) then centrifuged for 20 min at 20,000 × *g*. The supernatant was divided in to 250 µl aliquots and incubated with and without 1 µg SubAB at 4°C for at least 1 h. Samples were subsequently incubated with 2 µl mouse anti-His_6 mAb (Qiagen) at 4°C overnight and precipitated with 25 µl of 0.1 $mg.ml^{-1}$ protein G-Sepharose for Fast Flow (Amersham Biosciences, Piscataway, NJ) in Sol buffer at 4°C for 1 h. Beads were washed three times with PBS and proteins were solubilised by heating in 5 µl solubilising buffer (200 mM Tris [pH 6.8], 6% [w/v] SDS, 32% [v/v] glycerol, 0.32% [w/v] bromophenol blue). Samples were run in SDS-PAGE gels (Section 2.6.1) and transferred onto a nitrocellulose membrane as described in Section 2.6.6. A biotinylated protein ladder

(Cell Signaling Technology) was used as both a biotin control and an SDS-PAGE marker with sizes of 200, 140, 100, 80, 60, 50, 40, 30, 20 and 10 kDa.

2.11.2 Enhanced Chemiluminescence (ECL)

Membranes from Section 2.11.1 were blocked by incubating in 5% (w/v) skim milk powder in TTBS for 1 h with gentle shaking. Filters were then blotted with either streptavidin-HRP diluted 1:2,000 in blocking solution for 1 h with gentle shaking or anti-biotin-HRP (Cell Signaling Technology) diluted 1:1,000 in blocking solution at 4°C overnight. Blots were washed three times for 10 min with TTBS with gentle shaking then twice for 5 min with TBS with gentle shaking. Samples were detected using ECL by incubating membranes in Chemiluminescent Peroxidase Substrate-3 (Sigma) with excess fluid removed after 5 min. Chemiluminescence was detected by exposure of the membrane to X-ray film (AGFA, Mortsel, Belgium) and developed using an Curix 60 automatic X-ray film processor (AGFA).

2.12 Bacterial Receptor Mimic Constructs

2.12.1 LPS Receptor Mimic Preparation

CWG308 receptor mimic construct (RMC) bacterial strains were grown overnight and subcultured 1:20 with 1 mM IPTG at 37°C with shaking for 3 h. 1×10^9 bacteria were pelleted then resuspended in 50 µl lysing buffer (2% [w/v] SDS, 4% [v/v] β-mercaptoethanol, 10% [v/v] glycerol, 1 M Tris [pH 7.6], 0.1% [w/v] bromophenol blue) and boiled for 5 min. Samples were allowed to cool, incubated with 25 µg proteinase K (Roche) at 56°C for 4 h, diluted 1:4 in lysing buffer boiled for 5 min and stored at 4°C.

2.12.2 Toxin Overlay Assay (LPS Receptor Mimics)

5 µl of LPS receptor mimic samples prepared in Section 2.12.1 were run in pre-cast SDS-PAGE gels (Section 2.6.4) and transferred onto a PVDF membrane as described in Section 2.6.6. Membranes were then rinsed twice in TBS, blocked with TBS containing 10% (v/v) Blocking Reagent (Roche) for 1 h with shaking. After rinsing in TBS, membranes were overlaid with and without 1 $\mu g.ml^{-1}$ SubAB or SubAB-OG in 5% (v/v) Blocking Reagent in TBS at 4°C overnight.

PVDF sheets treated with SubAB were then washed three times for 10 min with TBS and incubated in mouse anti-His_6 mAb diluted 1:2,000 in blocking solution at 4°C overnight, washed with TBS as before, and incubated in goat anti-mouse IgG-AP diluted 1:4,000 in the blocking solution at 4°C overnight. Membranes were washed with TBS as before and developed as described in Section 2.10.5. Membranes treated with SubAB-OG were rinsed in TBS and imaged using a BioRad Molecular Imager FX (BioRad) with an excitation laser at 488 nm. Images were captured using Quantity One v4.3.1 build 003 (BioRad).

2.13 Receptor Structural Analysis

2.13.1 Mass Spectroscopy

Having identified putative SubAB receptor species determined by TLC toxin overlay assays (Section 2.10.5), corresponding regions of silica were scraped from the chromatogram and stored under nitrogen at –20°C. Scrapings were subsequently analyse by negative ion mass spectroscopy (MS), performed by Istvan Toth (Molecular and Microbial Sciences School, University of Queensland), and matrix-assisted laser desorption/ionisation MS (MALDI MS), performed by Peter Hoffmann (Adelaide Proteomics Centre, University of Adelaide).

2.13.2 Glycan Array

Glycan array analysis was performed by David Smith (CFG Core H, CA) in which, Version 2.1 of the printed array consisted of 285 oligosaccharides in replicates of six, incubated with 100 $\mu g.ml^{-1}$ of SubAB conjugated to Oregon Green 488 (Section 2.14.2). Maxima and minima were removed and thus, data are representative of four replicates indicating relative fluorescence units (RFU).

2.14 Fluorescence Materials

2.14.1 Coverslip Preparation

Round glass coverslips (13 mm diameter) were chemically etched by boiling for 1 min in 0.1 M HCl. After cooling to room temperature, coverslips were washed twice with MQ H_2O and once with methanol before storing in methanol at –20°C.

2.14.2 Fluorescent Toxins

SubAB and $SubA_{A272}B$ purified in Section 2.5 were labelled with FluoReporter Oregon Green 488 (OG) or Texas Red-X (TR) Protein Labelling Kits (Molecular Probes), according to the manufacturer's instructions, with a dye:protein molar ratio (MR) of 8:1. These will be referred to as SubAB-OG/-TR and $SubA_{A272}B$-OG/-TR, respectively. Purified StxB (a gift from Anne V. Kane, Division of Geographic Medicine and Infectious Diseases, Tufts New England Medical Centre, MA) was labelled using a FluoReporter TR Protein Labelling Kit with a dye:protein molar ratio of 8:1 and will be referred to as StxB-TR. Alexa Fluor 594-conjugated CtxB (CtxB-AF594) was purchased from Molecular Probes.

2.14.3 Intracellular Markers

Lysine fixable TR-conjugated 70,000 MW Dextran (Dextran-TR), TR-conjugated Transferrin (Tf-TR), TR-X-conjugated wheat germ agglutinin (WGA-TR),

mouse anti-Human Golgin-97 mAb (CDF4; Molecular Probes) and goat anti-BiP antisera (C-20; Santa Cruz Biotech, CA) were used to label endosomes, clathrin-coated pits, TGN/Golgi, Golgi and the SubA target, BiP respectively (Hopkins, 1983; Sandvig *et al.*, 1987; Mills and Finlay, 1994; Verma *et al.*, 2000; Khine *et al.*, 2004; Paton *et al.*, 2006a). LysoTracker DND-99, MitoTracker CMXRos and ER-Tracker Red (Molecular Probes) were used to label lysosomes, mitochondria and the ER, respectively. Rabbit anti-Prohibitin antisera (Neomarkers, CA) (a gift from Lesley Crocker, Molecular and Biomedical Sciences, University of Adelaide, Australia) was also used to label mitochondria. For detection, AF488-conjugated goat anti-mouse/-rabbit IgG (Molecular Probes) were used as were AF594-conjugated goat anti-mouse/-rabbit and donkey anti-goat IgG, as appropriate for the respective primary antibody.

2.14.4 Cell Cycle Markers

Polyclonal rabbit anti-Cyclin E (H-232) and anti-Cyclin B1 (M-20; Santa Cruz) were gifts from Josephine White (School of Molecular and Biomedical Science, University of Adelaide, SA, Australia) and were used to identify cells traversing G1 and G2 phases, respectively. Mouse anti-Phospho-Histone H3 (PH3) mAb (6G3; Cell Signaling Technology, MA) was used to identify mitotic cells while BrdU incorporation and subsequent detection with mouse anti-BrdU mAb (ZBU30; Invitrogen) was used to identify cells traversing S phase.

2.15 Toxin Trafficking by Fluorescence

2.15.1 Fluorescent Toxin Exposure

Vero cells harvested in Section 2.8.2 were diluted 1:5 and coverslips in 24-well trays were seeded with 250 µl of diluted cell suspension, made up to 1 ml with growth medium and grown to 50 – 75% confluence at 37°C overnight. Vero cells grown on

coverslips were washed with PBS and exposed to 0.5 μg.ml^{-1} CtxB-AF594 or StxB-TR or 1 μg.ml^{-1} fluorescent SubAB or SubA$_{A272}$B in tissue culture media at 37°C. After 30 min, unbound proteins were removed by washing with PBS and coverslips were subsequently incubated in growth media for the remainder of the desired time period, whereupon the cells were washed with PBS and fixed for at least 20 min in 4% (v/v) formaldehyde in PBS at 4°C. Coverslips were washed three times with PBS and twice with MQ H_2O and allowed to dry in the dark. Samples were mounted on glass slides in ProLong Gold Antifade reagent (Molecular Probes), cured overnight at room temperature and sealed with nail varnish.

2.15.2 Fluorescence Co-localisation

Vero cells exposed to SubAB-OG in Section 2.15.1 were simultaneously treated with 1 μg.ml^{-1} SubAB-TR, 0.5 μg.ml^{-1} StxB-TR or CtxB-AF594, 50 μg.ml^{-1} dextran-TR (to label endosomes), 5 μg.ml^{-1} Tf-TR (to label clathrin-coated pits) or 5 μg.ml^{-1} WGA-TR (to label *trans*-Golgi networks) for the first 30 min of the desired time period. For labelling of the mitochondria, the media was supplemented with 100 nM LysoTracker DND-99, 400 nM MitoTracker CMXRos or 1 μM ER-Tracker Red for the final 30 min of the desired time point. Samples were viewed by dual-laser confocal microscopy (Sections 2.16.2 and 2.16.3).

2.15.3 Immunofluorescent Co-localisation

For co-localisation with organelles labelled by immunofluorescence, Vero cells were initially exposed to SubAB-OG, washed and fixed as described in Section 2.15.1. Cells were subsequently permeabilised with 0.1% (v/v) Triton X-100 in PBS for 1 min, washed with PBS and blocked with 20% FCS (v/v) in PBS at 37°C for 1 h. Samples were incubated in blocking solution supplemented with 0.5 μg.ml^{-1} of mouse anti-

Human Golgin-97 (to label Golgi), goat anti-BiP (ER) or rabbit anti-Prohibitin antisera (mitochondria) at 37°C for 1h and then washed three times with PBS. For detection, coverslips were treated with the appropriate AF594-conjugated IgG diluted 1:200 in blocking solution at 37°C for 1 h. Coverslips were washed with PBS and MQ H_2O, dried, mounted, cured and sealed as described in Section 2.15.1. Samples were viewed by dual-laser confocal microscopy (Sections 2.16.2 and 2.16.3).

2.15.4 Cell Cycle Analysis

To identify toxin internalisation with respect to the cell cycle, Vero cells were exposed to SubAB-OG, CtxB-AF594 or StxB-TR for 30 min, then washed and fixed as described in Section 2.15.1. Vero cells in G1 and G2 phases were labelled by immunofluorescence with rabbit anti-Cyclin E and B1, respectively as detailed in Section 2.15.3. Mitotic cells were identified by nuclei harbouring Phospho-Histone H3 in which cells were simultaneously permeabilised and blocked with 0.1% (v/v) Triton X-100 and 20% FCS (v/v) in PBS at 37°C for 1 h. Samples were then incubated in mouse anti-PH3 diluted 1:400 in the aforementioned permeabilising/blocking solution at 37°C for 1h. After washing three times with PBS, coverslips were treated with AF488- or AF594-conjugated goat anti-mouse IgG in the permeabilising/blocking solution at 37°C for 1 h. Coverslips were washed with PBS and MQ H_2O, dried, mounted, cured and sealed as described in Section 2.15.1. Cells traversing the stages of mitosis were subsequently identified on the basis of chromosomal configuration.

For cells in S phase, Vero cells were grown in media containing fluorescent toxin supplemented with 20 µM BrdU for 30 min, formalin fixed at 4°C for 20 min and rinsed twice in wash buffer (0.1% [v/v] Triton X-100 in PBS). DNA was denatured for 30 min with 2 M HCl in wash buffer and neutralised with 0.1 M sodium tetraborate 10-hydrate. Samples were blocked with 20% FCS in wash buffer at 37°C for 1 h and

incubated with mouse anti-BrdU mAb diluted 1:400 in the blocking solution. For detection, samples were incubated with the appropriate AF488- or AF594-conjugated secondary antibody diluted 1:200 in the blocking solution, while SubAB-OG was resuscitated with AF488-conjugated goat anti-FITC/OG, as required. Samples were viewed by dual-laser confocal microscopy (Sections 2.16.2).

2.16 Fluorescence Microscopy

2.16.1 Epifluorescence Microscopy

Samples were initially viewed using an SPlan Apo 60 × 1.4 numerical aperture oil immersion lens in an Olympus IMT-2 inverted microscope fitted with epifluorescence optics. Optimum fluorochrome absorption and emission data are presented in Table 2.5; fluorochromes were visualised using a Hg-arc lamp and one of the two wide band filters as listed in Table 2.6.

Table 2.5: Fluorochrome optimum absorption and emission wavelengths.[a]

NOTE:
This table is included on page 50 of the print copy of the thesis held in the University of Adelaide Library.

[a] Adapted from Handbook of Fluorescent Probes and Research Products, 10th Ed. (Molecular Probes).

Table 2.6: Epifluorescence optics fitted to Olympus IMT-2 microscope.[a]

Fluorochrome	Filter block model (manufacturer)	Excitation λ(nm)	Emission filter λ (nm)
Green	Interference blue (Olympus)	450 – 470	Not provided
Red	41004:HQTR (Chroma)	535 – 580	605 – 670

[a] Adapted from Olympus and Chroma catalogues.

2.16.2 Dual-Laser Fluorescence Confocal Microscopy

Dual-laser confocal microscopy was performed using the above Olympus IMT-2 microscope coupled to a BioRad MRC-600. Fluorochromes were visualised with a 15 mW Krypton/Argon-mixed gas laser with lines at 488 nm and 568 nm of approximately 5 mW each. Filter sets were supplied by the manufacturer as described in Table 2.7.

Table 2.7: Optics fitted to BioRad MRC-600.[a]

NOTE:
This table is included on page 51 of the print copy of the thesis held in the University of Adelaide Library.

[a] Adapted from BioRad MRC-600 Operating Manual.

2.16.3 Image Acquisition and Analysis

All images were acquired using an SPlan Apo 60 × 1.4 numerical aperture oil immersion lens in the Olympus-BioRad MRC-600 dual-laser confocal microscope described in Section 2.16.2. The confocal aperture was set one third open and 8-bit images were captured using CoMOS v7.1 (Bio-Rad). Images were coloured and overlaid using Adobe Photoshop CS with pixel intensities adjusted so minimal and maximal values were ~0 and 255, respectively in each channel. Quantification of co-localisation was performed essentially as described by Nichols *et al.* (2001) where

ImageJ v1.38a (National Institutes of Health) was used to perform operations on binary images.

2.17 Toxin Trafficking by Electron Microscopy

2.17.1 LR White Resin Embedding

Cells grown to 90% confluence in a 75-cm^2 flask were washed twice with PBS and exposed to 5 $\mu g.ml^{-1}$ SubAB in tissue culture media at 37°C. After 30 min, non-adherent species were removed by washing with PBS and incubated in growth media until the desired time point. Cells were trypsinised as described in Section 2.8.2, harvested in the appropriate medium and pelleted at 400 × *g*. The sample was fixed at 4°C for 1 h in 4% (v/v) paraformaldehyde, 0.25% (v/v) glutaraldehyde and 4% (w/v) sucrose in PBS (pH 7.2) and washed twice in washing buffer (4% [w/v] sucrose in PBS) for 10 min. Cells were dehydrated by resuspending in three 20-min changes each of 70% (v/v), 90% (v/v), 95% (v/v) and finally 100% ethanol at 4°C. Cells were infiltrated with resin by resuspending in 50% (v/v) LR White hard grade acrylic resin (London Resin Company, London, England) in ethanol for 3 h and then in three 8-h changes of 100% LR White resin. Cells were embedded in fresh resin in gelatine capsules containing minimal air, pelleted and cured at 50°C for 36 h. 70-nm sections were cut and mounted on colloidin-coated nickel 200 mesh grids (ProSciTech, QLD, Australia) at Adelaide Microscopy (University of Adelaide).

2.17.2 LR White Resin Embedding in Transwells

1.2-mm diameter polycarbonate Transwell inserts with a 3 µm pore size (Corning Inc., Corning, NY) were seeded with ~5×10^4 Vero cells and grown overnight at 37ºC and treated with 5 $\mu g.ml^{-1}$ SubAB for 2 h in appropriate growth media. The upper chambers were fixed in PBS containing 4% sucrose (w/v), 4% paraformaldehyde

(v/v) and 0.25% glutaraldehyde (v/v) for 30 min, washed with 4% sucrose (w/v) in PBS then dehydrated in 70% (v/v), 90% (v/v), and 95% (v/v) ethanol changes for 10 min each and finally two 15-min changes of 100% ethanol. Inserts were infiltrated with LR White Resin (ProSciTech) by incubating in 50% LR White hard grade acrylic resin in ethanol for 30 min then in two 30-min changes of 100% resin. Membranes were peeled from the inserts, embedded in gelatine capsules filled with LR White and cured at 50ºC for 24 h. 70-nm sections were cut and mounted on colloidin-coated nickel 200 mesh grids (ProSciTech) at Adelaide Microscopy.

2.17.3 Epon Resin Embedding

Embedding in epon was performed essentially as described by van Deurs *et al*. (1986) and Sandvig *et al*. (1992) Cells grown to 90% confluence in a 75-cm^2 flask were washed twice with PBS and exposed to 1 $\mu g.ml^{-1}$ SubAB conjugated to peroxidase (SubAB-POD; reacted using a POD Labelling Kit-NH_2 [Dojindo Molecular Technologies, Gaithersburg, Maryland] according to the manufacturer's instructions) in tissue culture media at 37°C. After 1 h cells were fixed with 2.5% glutaraldehyde at room temperature for 1 h, gently washed with PBS and developed with 2 ml PBS containing 1 mg diaminobenzidine (DAB) and 2 µl 15% H_2O_2 at room temperature for 30 min. Cells were detached with a rubber policeman (BD Falcon), pelleted at 1,600 × *g* for 25 min and resuspended in 2% (w/v) OsO_4 at 4°C for 1 h. Cells were pelleted, treated with 1% uranyl acetate (v/v) at room temperature for 1 h, pelleted and resuspended in PBS containing 4% (w/v) sucrose for 10 min.

Cells were subsequently dehydrated by resuspending twice in 70% (v/v) and 90% (v/v) ethanol and once in 95% (v/v) ethanol for 10 min each and finally in three 10-min changes of 100% ethanol. Samples were infiltrated with epon resin (ProSciTech) by resuspending in 50% resin in ethanol for at least 40 min then in two

60-min changes of 100% resin. Cells were embedded in 1.5 ml plastic centrifuge tubes filled with epon and cured at 70ºC for 24 h. 70-nm sections were cut and mounted on colloidin-coated nickel 200 mesh grids (ProSciTech) at Adelaide Microscopy.

2.17.4 Immunogold Labelling of Resin Sections

Grids containing resin sections prepared in Sections 2.17.1and 2.17.2 were placed on a drop of 20 mM glycine (Sigma) for 20 min and blocked with 1% (w/v) ovalbumin (OVA; Sigma) in PBS for 20 min. Samples were treated with rabbit anti-SubA (Hui Wang, School of Molecular and Biomedical Science, University of Adelaide) diluted 1:100 in blocking solution overnight at 4°C, rinsed six times for 5 min in blocking solution and subsequently treated with Protein-A Gold complex diluted 1:100 in blocking solution for 90 min, rinsed six times for 5 min as before and washed in four large volumes of MQ H_2O.

2.17.5 Heavy Metal Staining of Resin Sections

Grids containing immunogold-labelled sections prepared in Section 2.17.4 were placed on a drop of 3% (v/v) uranyl acetate in 70% (v/v) ethanol for 10 – 20 min, dipped six times into each of three large volumes of MQ H_2O then placed on a drop of 2.6% (w/v) lead nitrate, 3.6% sodium citrate and 160 mM NaOH for 5 min in a covered petri dish containing NaOH pellets to absorb atmospheric CO_2 and washed as before. Samples were stored coated-side up on Whatman filter paper.

2.17.6 Transmission Electron Microscopy (TEM)

Grids were viewed using a Philips CM100 transmission electron microscope (Adelaide Microscopy) at an acceleration voltage of 80 kV. Images were captured using analySIS Pro version 3.1.b540 (Soft Imaging System GmbH, Münster, Germany) using a MegaView II camera (Soft Imaging System).

2.18 Inhibition of SubAB Trafficking and Cytotoxicity

2.18.1 Inhibition of SubAB Trafficking

Vero cells grown on coverslips in a 24-well tray as described in Section 2.15.1 were pre-incubated for 30 min at 4°C or at 37°C in media supplemented with 60 mM acetate (pH ~5), 1.5 $\mu g.ml^{-1}$ nocodazole, 25 $\mu g.ml^{-1}$ CPZ, 1.25 µM PAO, 1.25 $\mu g.ml^{-1}$ filipin, 100 $\mu g.ml^{-1}$ genistein, 5 mM MβCD or 0.5 $\mu g.ml^{-1}$ BFA, and then exposed to 1 $\mu g.ml^{-1}$ SubAB-OG for 3 h while maintaining the respective inhibitor.

2.18.2 Inhibition of Cytotoxicity

Vero cells harvested in Section 2.8.2 were diluted 1:5. Vero cell monolayers were grown by seeding 24-well trays with 500 µl of diluted cell suspension per well, made up to 1 ml with growth medium and grown in a humidified incubator with 5% CO_2 at 37°C overnight. Monolayers were pre-incubated for 30 min at 4°C or at 37°C in media supplemented with 60 mM acetate (pH ~5), 1.5 $\mu g.ml^{-1}$ nocodazole, 12.5 $\mu g.ml^{-1}$ CPZ, 1.25 µM PAO, 1.25 $\mu g.ml^{-1}$ filipin, 100 $\mu g.ml^{-1}$ genistein, 5 mM MβCD or 0.5 $\mu g.ml^{-1}$ BFA, and then exposed to 1 $\mu g.ml^{-1}$ SubAB for 3 h while maintaining the respective inhibitor. Cells in each well were subsequently solubilised in 100 µl 2 × LUG buffer (2% [w/v] SDS, 5% [v/v] β-mercaptoethanol, 10% [v/v] glycerol, 6.25 mM Tris [pH 6.8], 0.005% [w/v] bromophenol blue) and stored at –20°C. Samples were then subjected to SDS-PAGE (Section 2.6.1), transferred onto nitrocellulose (Section 2.6.2) and probed with anti-BiP (Section 2.6.3).

2.19 SubB Immunomodulation

2.19.1 Antigen Preparation

Antigens $SubA_{A272}$ or OVA were prepared with aluminium hydroxide adjuvant (Alum), CtxB, SubB or PBS. Antigens were formulated with Alum at a final ratio of

100 µg antigen to 1 mg Alum adjuvant. Antigens were first diluted in sterile PBS, such that after further addition of Alum, a final antigen concentration of 100 $\mu g.ml^{-1}$ was achieved. One fifth of the total Alum required was added every 10 min while agitating the mixture with a magnetic stirrer. The mixture was then agitated with a magnetic stirrer for a further 30 min, then made up to 150 µl per dose with PBS and stirred for at least 2 h. For toxin B subunits, antigens were admixed with 0.7143 nmol SubB (10 µg) or CtxB (8.285 µg) per dose, allowed to stand for 30 min, and then made up to 150 µl with PBS.

2.19.2 Preparation of Immune Sera

Groups of five male Balb/C mice (5 – 6 weeks old) were immunised by intraperitoneal (i.p.) injection of 150 µl volumes containing the indicated amount of antigen. Three immunisations were performed, spaced 14 days apart. Fourteen days after the final immunisation, mice were exsanguinated by cardiac puncture and blood was allowed to coagulate at 4°C overnight. After centrifugation at 800 × *g*, sera were separated and stored at –80°C in aliquots.

2.19.3 Enzyme-Linked Immunosorbent Assay

Enzyme-linked immunosorbent assays (ELISA) were performed in 96-well flat-bottomed Maxisorp Nunc-immuno plates (Nunc, Roskilde, Denmark). Trays were coated with 100 µl of Tris-saline azide (TSA; 25 mM Tris, 132 mM NaCl, 0.05% [w/v] NaN_3, pH 7.5) containing 5 $\mu g.ml^{-1}$ of either $SubA_{A272}$ or OVA at 4°C overnight then washed five times with ELISA wash buffer (5 mM Tris, 150 mM NaCl, 0.1% [v/v] Triton X-100, 3.6 mM HCl, pH 7.6) using an ELx50 automatic strip washer (Bio-Tek Instruments Inc., Winooske, VA), then blocked with 150 µl 1% (w/v) premium grade bovine serum albumin (BSA) (Trace Biosciences, Hamilton, New Zealand) at 37°C for

2 h. After washing as before, wells were treated with murine sera (Section 2.19.2) diluted 1:4,000 in BSA-Tween (0.8% [w/v] NaCl, 12.5 mM triethanolamine, 0.05% [v/v] Tween-20, 0.02% [w/v] NaN_3, 0.02% [w/v] BSA) while control sera were diluted 1:200. Antisera were subsequently serially diluted two-fold in BSA-Tween and incubated at 4°C overnight. Trays were then washed as before and treated with ELISA grade rabbit anti-mouse-AP (BioRad) diluted 1:15,000 in BSA-Tween at 4°C overnight. After washing as before, wells were developed in 100 µl substrate buffer (10.5% [w/v] diehtanolamine, 0.02% [w/v] NaN_3, 1 mM $MgCl_2$, 150 mM HCl, pH 9.8) containing 1 $mg.ml^{-1}$ 4-nitrophenyl phosphate disodium salt hexahydrate (Sigma) at 37°C and A_{405} read using a SpectraMax M2 spectrophotometer (Molecular Devices, Sunnyvale, CA).

Absorbance above background was plotted against serum dilution using Prism 5.01 (GraphPad Software, San Diego, CA) and the ELISA titre was defined as the reciprocal of the serum dilution resulting in an A_{405} reading of 0.2 above background. Data represent each mouse with corresponding means and significance was determined by a Student's *t*-Test on $\log_2$(titre).